GOETHE UNIVERSITÄT
FRANKFURT AM MAIN

The role of the selective autophagy receptor p62 in acute myeloid leukemia

Dissertation

zur Erlangung des Doktorgrades

der Naturwissenschaften

vorgelegt beim Fachbereich

Biochemie, Chemie und Pharmazie

der Johann Wolfgang Goethe-Universität

in Frankfurt am Main

von

The Duy Nguyen

aus Ho Chi Minh Stadt, Vietnam

Frankfurt (2017)

(D 30)

vom Fachbereich Biochemie, Chemie und Pharmazie der

Johann Wolfgang Goethe-Universität als Dissertation angenommen.

Dekan: Prof. Dr. Clemens Glaubitz

Gutachter: Prof. Dr. Rolf Marschalek

                Prof. Dr. med. Christian Brandts

Datum der Disputation:

Table of contents

Table of contents

Table of contents

List of figures

List of figures

List of tables

1. Introduction

1.1 Acute myeloid leukemia

During leukemogenesis hematopoietic stem cells (HSC) accumulate transforming genetic and epigenetic alterations. In human and murine embryogenesis HSCs are derived from the yolk sac, dorsal aorta, fetal liver and placenta. Around the time of birth, HSCs migrate to the bone marrow (BM), where they reside throughout the lifetime of the organism (Mikkola and Orkin, 2006). HSCs are able to self-renew and differentiate into all blood lineages through hierarchical progenitor stages (Weissman, 2000). During leukemogenesis, HSCs reprogram their metabolic machinery to escape cell death, become autonomous and acquire new invasive properties.

Acute myeloid leukemia (AML) is a clonal malignancy characterized by expansion of undifferentiated myeloid blasts in the bone marrow interfering with production and function of normal blood cells. Consequently, deficiency of white blood cells (leukopenia) results in increased susceptibility to infection, drop of red blood counts (anemia) leads to fatigue and lack of platelets (thrombocytopenia) impairs the blood clotting. Based on diagnostic algorithms including morphology, immunophenotype, cytochemical staining, genetic features and clinical information, AML is classified according to *World Health Organization Classification of Tumours of Haematopoietic and Lymphoid Tissues*. The main categories are AML with recurrent genetic abnormalities, AML with myelodysplasia-related changes, therapy-related AML, and AML not otherwise specified (Arber et al., 2016).

AML is the most common acute leukemia in adults with an incidence of 3-4 cases per 100.000 people per year (Schlenk, 2014). AML progresses rapidly and fatally within weeks or months. Although around 40% of AML patients below the age of 60 years are cured, the prognosis for the majority of the patients remains poor and relapse frequently occurs (Dohner et al., 2015). Therapeutic strategies for AML have not been changed widely in more than 30 years. The standard (classical) treatment of most AML types remains chemotherapy given right after diagnosis. Notably, 60% to 85% of younger

adults (18 to 60 years old) reach complete remission (CR). However, CR rate is significantly lower in patients older than 60 years of age (40 to 60%) (Dohner et al., 2015). After achieving first remission, it has been shown that all patients relapse without further treatment (Cassileth et al., 1988). Therefore, post-remission therapies are applied to prevent relapse including high dose chemotherapy, maintenance therapy and hematopoietic stem cell transplantation (Dohner et al., 2010).

Based on our scientific understanding on the biological, genetic and epigenetic causes of leukemia, a plethora of novel therapeutic compounds have been developed to treat AML. These drugs target chromatin regulators, antigens expressed on leukemic blasts or essential signaling pathways in AML (Dohner et al., 2015). Specifically, the role of cellular degradation pathway known as autophagy is currently highlighted in the leukemogenesis of AML including increased self-renewal, proliferation, survival and response to chemotherapy (Auberger and Puissant, 2016). Little is known about this important cellular process in normal and malignant hematopoiesis, in particular in AML.

1.2 Autophagy

1.2.1 Mechanism of autophagy

Autophagy (meaning "self-eating" in Greek) was first termed by the Nobel laureate Christian de Duve in 1963 (Klionsky, 2008) and was described as a catabolic degradation process for intracellular components within lysosomes (Mizushima, 2007). Three different types of autophagy have been identified: microautophagy, chaperone-mediated autophagy (CMA) and macroautophagy. Microautophagy and CMA incorporate cytoplasmic cargoes directly into the lysosome for degradation. Macroautophagy (herein referred to as autophagy) engulfs proteins, macromolecular aggregates and damaged organelles within specific double-membrane vesicles called autophagosomes. Autophagosomes subsequently fuses with a lysosome to

1. Introduction

form autolysosome where sequestered cargoes are degraded (Levine and Kroemer, 2008).

The autophagic pathway is a multistep process hierarchically controlled by more than 30 autophagy-related genes (ATG) and consists of different phases: initiation, elongation, lysosomal fusion and degradation (Figure 1). Mammalian target of rapamycin (mTOR) complex is a key regulator of autophagy cascade controlling the induction phase to orchestrate the autophagosomes formation (Noda et al., 2009). Under nutrient-rich conditions, activated mTOR inhibits the protein kinase ULK1 complex activity, leading to autophagy inhibition. Under cellular stress such as starvation, protein aggregation, ROS accumulation (caused by damaged mitochondria) or pathogen invasion, mTOR is inhibited, which causes activation of the ULK1 complex and induction of autophagy. Initiation of autophagosome formation starts with phosphorylation of Beclin1 (BECN1) by ULK1 (Russell et al., 2013), which subsequently activates a core complex containing Beclin1 and the class III phosphatidylinositol-3 kinase Vps34 to facilitate vesicle nucleation (Funderburk et al., 2010). Autophagosomal elongation and maturation are mediated by two ubiquitin-like systems (UBLs): the ATG12-ATG5-ATG16L and MAP1LC3 (microtubule associated protein 1 light-chain 3, hereafter referred to as LC3) modifiers. The UBLs ATG12 and LC3 have functional similarities to the ubiquitin system as both utilize the E1-like enzyme ATG7 for their activation (Mizushima, 2007). Consequently, conjugation of the cytosolic LC3 (LC3-I) to phosphatidylethanolamine (PE) is mediated by the E2-like enzyme ATG3 and E3-like complex ATG12-ATG5-ATG16L. This leads to formation of LC3-phosphatidylethanolamine (LC3-II), which is translocated to the membrane of the autophagosomes (Shaid et al., 2013) (Figure 1). LC3 in turn stimulates the autophagosome formation and fusion with lysosomes into autolysosomes (Karanasios et al., 2016). Finally, the degradation of the inner autophagosomal membrane by lysosomal enzymes releases the enclosed cytoplasmic contents and accomplishes the degradation process.
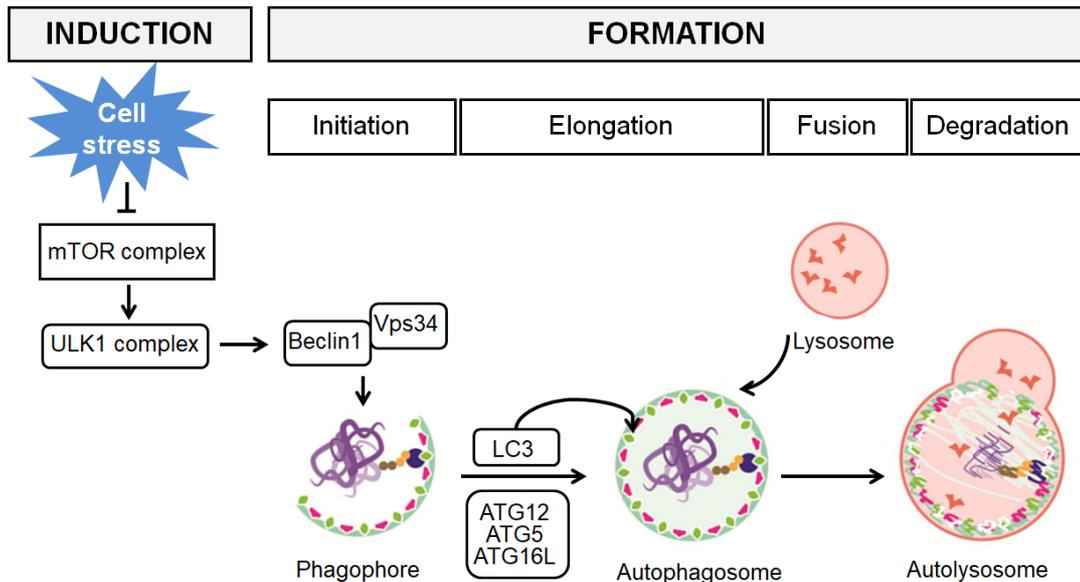
Figure 1. Schematic depiction of the induction and formation of autophagy. Autophagy is induced upon cellular stresses such as starvation, protein aggregation, ROS accumulation (caused by damaged mitochondria) or pathogen invasion. This leads to inhibition of the mTOR complex, which subsequently activates the ULK1 complex. ULK1 in turn phosphorylates Beclin1 to form the Beclin1-Vps34 complex initiating the formation of the phagophore. In the next step, the phagophore expands into a double-membrane vacuole called autophagosome. This process is mediated by 2 UBLs, the ATG12-ATG5-ATG16L and LC3, to conjugate LC3 into the membrane of the autophagosome. Afterwards, autophagosome fuses with a lysosome to form an autolysosome. Finally, the autophagosomal content is degraded within autolysosome. Figure modified from (Shaid et al., 2013).

1.2.2 Autophagy in cancer

As a key regulator in maintaining cellular homeostasis, autophagy plays a dual role in cancer. During cancerogenesis, autophagy has a tumor suppressive function by forming a robust barrier against malignant transformation. However, in established tumor, autophagy supports cancer cell growth and survival in response to starvation, hypoxia and cytotoxic drugs (Galluzzi et al., 2015).

Previous reports have shown that deletion of essential autophagy genes promotes malignant transformation. For example, heterozygous deletion of Beclin1 in mice leads to the development of spontaneous malignancies such as lymphomas, liver and lung cancer (Qu et al., 2003). Furthermore, depletion of ATG7 or ATG5 in mouse liver results in benign hepatic adenomas (Takamura et al., 2011). Similarly, ATG7 deletion in lung accelerates BRAF(V600E)-induced lung carcinomas (Strohecker et al.,

2013). Moreover, loss of ATG5 in lung enhances KRAS(G12D)-induced lung carcinomas caused by accumulation of dysfunctional mitochondria, oxidative stress and DNA damage (Rao et al., 2014). The same phenomenon has been also observed upon loss of ATG7 in murine HSCs as elevated mitochondrial ROS (reactive oxygen species) due to impaired autophagy leads to a myeloproliferative disorder in mice. Malignant transformation was mainly caused by ROS-induced DNA damage, indicating that autophagy protects healthy cells from genotoxicity, which otherwise would provoke tumorigenesis (Mortensen et al., 2011).

On the other side, it has been demonstrated that autophagy contributes to cancer progression in established tumors, while high autophagic activity is associated with poor outcome, metastatic potential and proliferation in various cancer types (Lazova et al., 2012). Other studies reveal that suppression of autophagy impairs tumor progression. For instance, loss of ATG7 in established BRAF(V600E)-induced lung tumor reduces proliferation and tumor burden accompanied with impaired mitochondrial metabolism, which seems to be critical for tumor growth (Strohecker et al., 2013). Similar effects have been observed in other cancer types after inhibition of autophagy such as KRAS(G12D)-induced lung tumor (Rao et al., 2014), pancreatic tumor (Rosenfeldt et al., 2013; Yang et al., 2014) and breast carcinoma (Huo et al., 2013).

Taken together, these studies propose that autophagy counteracts the metabolic stress which established tumor undergo and therefore plays an essential role in cancer maintenance and progression (Galluzzi et al., 2015).

1.3 Selective autophagy

In the past, autophagy was considered to be a bulk process. More recently, a plethora of intracellular cargoes were found to be degraded with high selectivity (Johansen and Lamark, 2011). Furthermore, selective autophagy has been linked to various human diseases ranging from infectious disease to neurodegenerative disorders and cancer (Komatsu and Ichimura, 2010;

Mizumura et al., 2014). Similar to bulk autophagy, selective autophagy can be activated by distinct external stimuli such as nutrient deprivation or cellular stresses (i.e. oxidative, osmotic and hypoxic) (Farre and Subramani, 2016). However, besides the core autophagy machinery apparatus, selective autophagy requires additional adaptor proteins (receptors) which mark specific cargo for autophagic degradation. Although the defined mechanism of cargo recognition still remains unclear, it is well established that ubiquitination is involved in this process (Shaid et al., 2013). Selective autophagy receptors "tether" the ubiquitinated cargoes to the nascent autophagosome by the presence of a LC3-interaction region (LIR), which binds LC3 on the surface of autophagosomes (Weidberg et al., 2011) (Figure 2). Thus, selective autophagy receptors allow diverse cellular regulation and thereby serve as a cellular quality control mechanism.
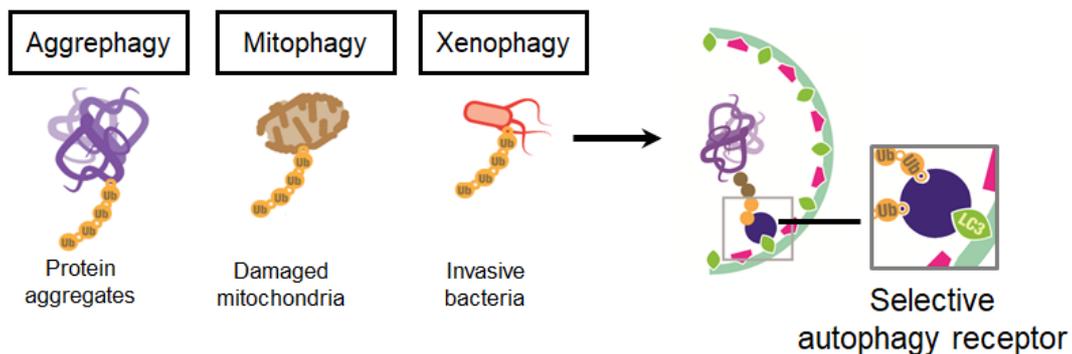
Figure 2. Mechanism of selective autophagy. Selective autophagy serves as a cellular quality control mechanism, in which cytoplasmic cargos such as protein aggregates, damaged mitochondria or invasive bacteria are selectively degraded by autophagy. As the first step, the cargos are ubiquitinated. Afterwards, specific proteins called selective autophagy receptors bridge the ubiquitinated cargos onto the membrane of the autophagosomes. Figure modified from (Shaid et al., 2013).

1.3.1 Selective autophagy receptors

Selectivity in autophagy depends on autophagy receptors which mediate elimination of different intracellular cargos such as mitochondria (mitophagy), protein aggregate (aggrephagy), peroxisome (pexophagy), ribosomes (ribophagy), endoplasmic reticulum (ER-phagy) and invasive bacteria (xenophagy) (Johansen and Lamark, 2011) (Figure 2).

1. Introduction

The first identified autophagy receptor was sequestosome 1 (p62/SQSTM1, referred to as p62), which has been extensively studied. Up to date, p62 is involved in numerous types of selective autophagy including aggrephagy (Bjorkoy et al., 2005; Pankiv et al., 2007), mitophagy (Geisler et al., 2010), pexophagy (Zhang et al., 2015) and xenophagy (Dupont et al., 2009). As an interaction partner of p62 (Lamark et al., 2003), neighbor of BRCA1 (NBR1) has been identified as the second autophagy receptor in aggrephagy (Kirkin et al., 2009b). Similar to p62, NBR1 also mediates pexophagy, although it functions independently from its interaction partner, underlining that autophagy receptors can share certain cargoes and have redundant functions. This is also applied to other autophagy receptors, as optineurin (OPTN) and calcium-binding and coiled-coil domain-containing protein 2 (CALCOCO2/NDP52, hereafter referred as NDP52) were recently identified to be indispensable receptors for mitophagy (Heo et al., 2015; Lazarou et al., 2015) and xenophagy (Thurston et al., 2012; Wild et al., 2011).

To achieve selectivity in autophagy, molecular markers are required for recognition of the cargo by adaptor proteins. This implies that selective autophagy receptors have to be equipped with essential "recognition domains" to fulfil this function (Figure 3). From yeast to mammals all selective autophagy receptors binds ATG8/LC3 – crucial for autophagosome formation – via a highly conserved LIR (LC3-interaction region) motif (Birgisdottir et al., 2013). Consequently, this interaction mediates a direct transfer of the targeted cargoes into the autophagosome. The molecular mechanism of cargo recognition is still largely unknown and currently under investigation. However, the role of ubiquitin is clearly important, as several autophagy receptors possess an ubiquitin-binding domain (UBD) to recognize autophagic targets. Three UBDs have been discovered until now: i. ubiquitin-associated domain (UBA) in p62 and NBR1, ii. ubiquitin binding domain in ABIN, NEMO (UBAN) and OPTN and iii. ubiquitin-binding zinc finger domain (UBZ) in NDP52 (Figure 3) (Behrends and Fulda, 2012).

Besides UBDs, cargo recognition can occur independently from ubiquitination. It has been shown that the Phox and Bem1 (PB1) domain of

p62 and NBR1 can recognize, polymerize and interact with each other (Bjorkoy et al., 2005; Kirkin et al., 2009a). For instance, PB1-mediated p62 polymerization is known to be critical for clustering of defective mitochondria in Parkin-mediated mitophagy (Narendra et al., 2010a). Moreover, PB1 is crucial for targeting p62 into the autophagosome formation site (Itakura and Mizushima, 2011). Additionally, the mitochondrial protein BCL2/adenovirus E1B 19 kDa protein-interacting protein 3-like (BNIP3L), also known as NIX has been classified as a mitophagy receptor lacking a UBD domain (Novak et al., 2010). Ubiquitination is therefore not required for NIX-dependent mitophagy due to its physiological localization within the mitochondrial outer membrane.

INTERACTION WITH UBIQUITIN AND LC3	LIR MOTIF	INVOLVED IN
p62	DDWTHL	Aggrephagy, mitophagy, pexophagy, xenophagy
NBR1	EDYIII	Aggrephagy, pexophagy
OPTN	DSFVEI	Mitophagy, xenophagy
NDP52	EDILVV	Mitophagy, xenophagy

INTERACTION WITH LC3	LIR MOTIF	INVOLVED IN
NIX	SSWVEL	Mitophagy

Figure 3. Domain structure of several selective autophagy receptors. Listed are several selective autophagy receptors, their autophagy-dependent domains, the associated LIR motif sequence and the type of selective autophagy they are involved in. Selective autophagy receptors are classified into 2 categories: p62, NBR1, OPTN and NDP52 interact with ubiquitin via ubiquitin binding domain (UBA in p62 and NBR1, UBAN in OPTN and UBZ in NDP52) and LC3 via LIR motif; NIX interacts directly with LC3 via LIR motif without UBD. Numbers indicate the length of amino acid in human proteins. Figure modified from (Shaid et al., 2013).

1.3.2 Mitophagy

The engulfment of mitochondria in lysosome was firstly observed in rat liver cells using electron microscopy in 1962 (Ashford and Porter, 1962). In 2005 Lemasters J.J. coined the term mitophagy to describe the selective degradation of mitochondria by autophagy (Lemasters, 2005). Up to date, mitophagy has been described in various functions ranging from embryonic development to cellular quality control.

During spermatogenesis paternal mitochondria are ubiquitinated and eliminated after entering the oocyte's cytoplasm (Sutovsky et al., 1999).

1. Introduction

Interestingly, p62 has also been detected in the degraded part of the spermatozoon, implicating p62 as a receptor in post-fertilization mitophagy (Al Rawi et al., 2011). Mitophagy plays also an essential role in mitochondrial clearance during red blood cell differentiation (reticulocyte maturation). Importantly, it has been shown that the selective autophagy receptor NIX is indispensable for this process (Schweers et al., 2007).

On the other side, mitochondria serve as the main site of aerobic energy production in eukaryote generating ROS as a by-product during oxidative phosphorylation. Thus, imbalance of ROS caused by dysfunctional mitochondria disrupts cellular physiology and has been implicated in a variety of diseases including cancer (Auten and Davis, 2009; Murphy, 2013). Degradation of dysfunctional mitochondria by mitophagy is therefore essential for maintaining cellular homeostasis (Kim et al., 2007).

Mounting evidences indicate that mitochondrial membrane depolarization is the activating signal for mitochondrial degradation (Elmore et al., 2001; Tolkovsky et al., 2002). Subsequently, depolarized mitochondria are selectively segregated by fission and degraded by autophagy (Twig et al., 2008). Upon mitochondrial damage the mitochondrial kinase PINK1 is firstly stabilized on the outer membrane (MOM) and secondly recruits the cytosolic E3 ubiquitin ligase Parkin to the depolarized mitochondria (Narendra et al., 2010b). Parkin leads to the ubiquitination of several MOM proteins (Sarraf et al., 2013), which can be recognized by the mitophagy receptors OPTN, NDP52 and p62. Activation of those mitophagy receptors is tightly regulated by PINK1/Parkin mediated phosphorylation of the serine/threonine-protein kinase TBK1 (Heo et al., 2015).

However, it has been proposed that mitophagy is not only controlled by PINK/Parkin-mediated signaling pathway. For instance, Allen et al. showed that loss of iron causes mitochondrial dysfunction without affecting mitochondrial membrane potential. This leads to mitochondrial degradation by mitophagy independent of PINK1/Parkin activation. Interestingly, treatment with the iron chelator deferiprone (DFP) causes upregulation of

p62, suggesting its potential role in PINK1/Parkin-independent mitophagy (Allen et al., 2013).

1.4 The adapter protein p62

When the scaffold protein p62 has been originally discovered by Joung et al, it was characterized as a phosphotyrosine-independent interaction partner of p56(lck) containing a PEST motif, a G-protein binding region and a zinc finger motif (Joung et al., 1996). Later, its PB1 domain has been identified to interact with the atypical protein kinase C isoforms (aPKCs), which are associated with survival and proliferation. Interestingly, p62 co-localizes with aPKCs and epidermal growth factor receptors in lysosome-targeted endosomes, suggesting its role as a signaling hub controlling the growth factor trafficking (Sanchez et al., 1998).

1.4.1 The non-autophagy functions of p62

Beyond its role in selective autophagy, p62 is also involved in numerous key signaling pathways due to its multiple adaptor sites (summarized in Figure 4).

The nuclear factor-kappaB (NF-κB) signaling pathway plays a central role in inflammation (Piva et al., 2006). Early studies have shown that p62 associates with tumor necrosis factor (TNF) receptor associated factor 6 (TRAF6) via the TRAF6-binding (TB) domain. This interaction is required for NF-κB activation by interleukin 1 receptor and the nerve growth factor receptor (Sanz et al., 2000; Wooten et al., 2001). Thus, p62 can activate the expression of NF-κB-associated inflammatory genes regulating cellular survival (Duran et al., 2008).

The mammalian target of rapamycin (mTOR) signaling pathway is a central regulator of cell growth and proliferation by inhibition of catabolic processes including autophagy (Laplante and Sabatini, 2009). p62 has been shown to be involved in mTOR signaling by interaction with the regulatory-associated protein of mTOR (Raptor) and co-localization with Rags GTPase on the

lysosome in an amino-acid dependent manner (Duran et al., 2011). In addition, the kinase MEKK3 binds p62 via its PB1 domain leading to phosphorylation of p62 and thereby activating mTOR signaling (Linares et al., 2015). This suggests that p62 may regulate autophagy through mTOR inhibition in response to nutrient starvation (Duran et al., 2011).

The Keap1-Nrf2 pathway is essential for anti-oxidative response in cells. Under basal conditions (non-stressed), the adaptor protein Keap1 mediates the degradation of the transcription factor Nrf2 by the proteasome (Ichimura et al., 2013). In contrast, under cellular stress condition (i.e. increased ROS), p62 binds Keap1 through its Keap1-interaction region (KIR) domain. This leads to stabilization of Nrf2, which translocates to the nucleus and initiates an anti-oxidative transcriptional process. Importantly, this is accompanied by upregulation of p62 gene expression, indicating a positive feedback loop (Jain et al., 2010). Interestingly, the degradation of Keap1 by p62 is mediated by selective autophagy independently from the Keap1-Nrf2 pathway (Ichimura et al., 2013).
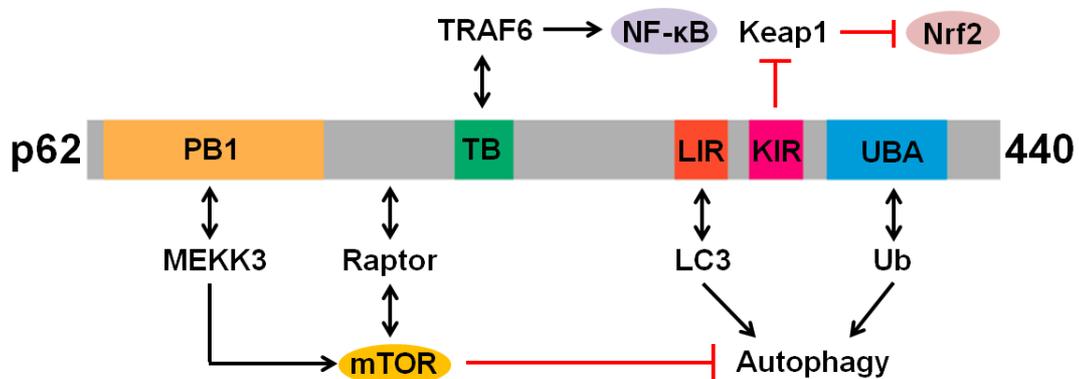
Figure 4. Structural domains and binding partners of p62. Schematic overview of the most important domains of p62 (PB1, TB, LIR, KIR, UBA) and their related binding partners (MEKK3, Raptor, TRAF6, LC3, Keap1, Ub), which regulates essential cellular signaling pathways including mTOR, NF-κB and Keap1-Nrf2. Figure modified from (Moscat et al., 2016).

1.4.2 p62 in cancer

As described, p62 acts at the interface between pro-oncogenic signaling pathways (NF-κB, Keap1-Nrf2, mTOR) and autophagic degradation

pathways. This emphasizes that p62 is a critical stress sensor, thereby controlling tumor initiation or suppression and progression.

During tumor initiation, p62 has been shown to be critical for Ras-induced lung cancer, which is involved in the NF-kB signaling pathway (Duran et al., 2008). Moreover, p62 accumulation caused by autophagy inhibition in response to metabolic stress triggers tumorigenesis, suggesting that autophagy eliminates p62 to suppress tumor growth (Mathew et al., 2009). Strikingly, Umemura et al. determined the oncogenic role of p62 by showing that overexpression of p62 in liver cells is sufficient to induce hepatocellular carcinoma (HCC) via Nrf2 and mTOR but not autophagy (Umemura et al., 2016). In established tumor, high p62 expression correlates with shorter survival in non-small cell lung cancer (Wang et al., 2015) and poor prognosis in epithelial ovarian cancer and endometrial cancer (Iwadate et al., 2014; Iwadate et al., 2015). These observations may suggest a tumor promoting role of p62 in cancer. It was reported that p62 has a pro-survival function in acute promyelocytic leukemia, and that this function depends on NF-κB activation (Trocoli et al., 2014).

2. Aims of the thesis

Malignant transformation of acute myeloid leukemia occurs at the hematopoietic stem cell stage due to genetic alterations. It has been demonstrated that impaired autophagy in murine HSCs causes accumulation of dysfunctional mitochondria and ROS, which promotes the development of a myeloproliferative disorder. This highlights the essential role of bulk autophagy in preventing malignant transformation by maintaining HSC integrity. However, it remains unknown how selective autophagy contributes to this process, especially which functional role autophagy receptors play in leukemogenesis. p62 has been identified as one of the first selective autophagy receptors, protecting cells from oxidative and genotoxic stress by removing deleterious organelles such as dysfunctional mitochondria or cytosolic components. Due to its multiple adaptor sites p62 is also involved in different pro-oncogenic signaling pathways in cancer.

This study aims to elucidate the role of p62 during AML development and maintenance by genetic modification of p62 expression in human und murine AML cell lines. By use of a murine p62 knockout AML transplantation model, we focused on the function of p62 as a selective autophagy receptor in malignant transformation, leukemia development and mitochondrial quality control.

3. Materials and methods

3.1 Materials

3.1.1 Reagents, cell culture media and kits

All reagents, cell culture media and kits used in this study were stored and prepared according to manufacturer's instruction, and are listed in Table 1.

Reagents, cell culture media and kits	Manufacturer
7-Aminoactinomycin D (7AAD)	BD Biosciences
Annexin V	BD Biosciences
Bovine serum albumin (BSA)	Sigma-Aldrich
Bafilomycin A1	LC Laboratories
BrdU Flow Kit	BD Biosciences
BlockAid solution	Life Technologies
Distilled water (DNase/RNase free)	Gibco
Dialyzed fetal bovine serum (FBS)	Invitrogen
DMEM medium	Gibco
DAPI	AnaSpec
Fetal calf serum (FCS)	Sigma-Aldrich
Glycine	Sigma-Aldrich
Iscove Basal Medium	Biochrom
Image-IT FX Signal Enhancer	Life Technologies
Lineage Cell Depletion Kit	Miltenyi Biotec
Methocult GF M3534	STEMCELL Technologies
MitoSOX™ Red mitochondrial superoxide indicator	Life Technologies
MES SDS Running Buffer (20x)	Life Technologies
Methanol	Sigma-Aldrich
Milk powder	Carl Roth
NaCl	Sigma-Aldrich

3. Materials and methods

NaF	Sigma-Aldrich
NP40	Sigma-Aldrich
Phosphate buffered saline (PBS)	Gibco
Penicillin and streptomycin (Pen Strep)	Sigma-Aldrich
Polyethylenimine (PEI)	Sigma-Aldrich
Puromycin	Sigma-Aldrich
Protease inhibitor cocktail	Roche
Protein A/G PLUS-Agarose beads	Santa Cruz
Prolong Diamond Antifade Mountant	Life Technologies
RPMI 1640 Medium	Gibco
RevertAid H Minus Reverse Transcriptase	Thermo Fisher Scientific
SILAC medium	Thermo Fisher Scientific
Sodium orthovanadate	Sigma-Aldrich
SuperSignal™ West Femto	Thermo Fisher Scientific
SYBR® Green JumpStart™ Taq ReadyMix	Sigma-Aldrich
Tris	Sigma-Aldrich
Tween® 20	Applichem
TRI Reagent®	Sigma-Aldrich
XF Cell Mito Stress Test Kit	Seahorse Bioscience
TurboFect Transfection Reagents	Thermo Fisher Scientific
Trypan Blue	Sigma-Aldrich

Table 1. List of reagents, cell culture media and kits

3.1.2 Cytokines

Cytokines (listed in Table 2) used in this study were dissolved at appropriate concentration in 10% distilled water (DNase/RNase free), 0.1% bovine serum albumin (BSA) and 89.9% Dulbecco's phosphate buffered saline (PBS), followed by sterile-filtered through 0.2µm diameter filter (Filtropur S 0.2, Sarstedt).

3. Materials and methods

Cytokines	Concentration	Manufacturer
Murine interleukin-3 (mIL-3)	10ng/ml	Peprotech
Murine interleuin-6 (mIL-6)	10ng/ml	Peprotech
Murine stem cell factor (mSCF)	50ng/ml	Peprotech

Table 2. List of cytokines

3.1.3 Antibodies

Antibodies used for Western Blot are listed in Table 3.

Antibodies	Species	Dilution	Type	Manufacturer
Anti-ß-actin	Mouse	1:10000	Primary	Sigma-Aldrich
Anti-COXIV	Rabbit	1:1000	Primary	Cell Signaling
Anti-LC3	Rabbit	1:1000	Primary	Novus Biologicals
Anti-p62/SQSTM1	Mouse	1:1000	Primary	Abnova
Anti-Tom20	Rabbit	1:1000	Primary	Santa Cruz
Anti-VDAC1	Goat	1:1000	Primary	Santa Cruz
Anti-mouse IgG-HRP	Goat	1:10000	Secondary	Jackson ImmunoResearch
Anti-rabbit IgG-HRP	Goat	1:10000	Secondary	Jackson ImmunoResearch

Table 3. List of antibodies used for Western Blot

Antibodies used for immunofluorescent staining are listed in Table 4.

Antibodies	Species	Dilution	Type	Manufacturer
Anti-LC3	Mouse	1:50	Primary	MBL International
Anti-Tom20	Rabbit	1:50	Primary	Santa Cruz
Anti-mouse IgG-AF594	Goat	1:300	Secondary	Invitrogen
Anti-rabbit IG-AF647	Goat	1:300	Secondary	Invitrogen

Table 4. List of antibodies used for immunofluorescent staining

3. Materials and methods

Antibodies used for flow cytometry (listed in Table 5) were diluted according to manufacturer's instruction.

Antibodies	Species	Conjugated	Manufacturer
Mouse Lineage Antibody Cocktail	Not stated	V450	BD Biosciences
Mouse Lineage Antibody Cocktail	Not stated	APC	BD Biosciences
Anti-mouse CD117 (cKit)	Rat	PE-Cy™7	BD Biosciences
Anti-mouse CD117 (cKit)	Rat	APC	BD Biosciences
Anti-mouse Ly-6A/E (Sca1)	Rat	V450	BD Biosciences
Anti-mouse CD34	Rat	FITC	BD Biosciences
Anti-mouse CD135 (Flt3)	Rat	PE	BD Biosciences
Anti-mouse Ly-6G and Ly-6C (Gr1)	Rat	APC	BD Biosciences
Anti-mouse CD11b	Rat	PE	BD Biosciences
Anti-mouse CD16/32	Rat	PerCP/Cy5.5	Biolegend

Table 5. List of antibodies used for flow cytometry

3.1.4 Instruments, incubators and microscopes

All instruments, incubators and microscopes used in this study are listed in Table 6.

Instruments, incubators and microscopes	Manufacturer
Animal Blood Counter	scil animal care company GmbH
BD FACSAria III	BD Biosciences
BD LSRFortessa™	BD Biosciences
Cell Culture Microplate	Seahorse Bioscience
DNA Engine Opticon 2 Real-Time Cycler	Bio-Rad
Heracell 150i incubator	Thermo Fisher Scientific
Leica TCS SP5 II	Leica Microsystems
Mastercycler pro	Eppendorf

NanoDrop 2000c Spectrophotometer	Thermo Fisher Scientific
Odyssey FC imaging system	LI-COR Biosciences
Seahorse XF96 Extracellular Flux Analyzer	Seahorse Bioscience
XCell SureLock™ Mini-Cell Electrophoresis System	Invitrogen

Table 6. List of instruments, incubators and microscopes

3.1.5 Cell culture

Human AML cell lines THP1, U937, Molm13 and NB4 (purchased from Leibniz-Institut DSMZ-Deutsche Sammlung von Mikroorganismen und Zellkulturen GmbH, Braunschweig, Germany) were cultured in RPMI 1640 Medium (Gibco) supplemented with 10% heat-inactivated fetal bovine serum (FBS) and 1% penicillin/streptomycin (Pen Strep). Murine MN1-driven ldMBM leukemia cells were cultured in Iscove Basal Medium supplemented with 10% heat-inactivated FBS, 1% penicillin/streptomycin and following cytokines: 50ng/ml murine stem cell factor (mSCF), 10ng/ml murine interleukin-3 (mIL-3) and 10ng/ml murine interleukin-6 (mIL-6). Plat-E and HEK293T cells (DSMZ) were cultured in DMEM medium (Gibco) containing 10% heat-inactivated FBS and 1% penicillin/streptomycin. All cell lines were cultured at 37^oC with 5% CO_2 in a humidified Heracell 150i incubator.

3.1.6 Mice

$p62^{-/-}$ mice were kindly provided by the Dikic laboratory. Wild-type C57BL/6J (6- to 12-week-old) mice were purchased from JANVIER LABS (Mayenne, France). All mice were kept under pathogen-free conditions in the research animal facility of the University Hospital Frankfurt according to institutional guidelines. All animal experiments were approved by the official committee on animal experimentation (Regierungspräsidium Darmstadt).

3.2 Methods

3.2.1 *In silico* analysis of p62 expression in human AML patients

RNA sequencing data (normalized RSEM values) from the LAML project (Ley et al., 2013) were analyzed on the IlluminaHiSeq_RNASeqV2 platform (aligned against hg19) and clinical data were accessed from the GDC legacy archive on 20.08.2017 using TCGAbiolinks (Colaprico et al., 2016). Clinical data included in the analysis were vital status and time-to-event (equals to days to death if patient died, or if a patient is alive equals to days to last follow-up). Cases with right-censored time-to-event data were included in the analysis. Data was analyzed using R and graphs were created with ggplot2. The log rank test implemented in R's survdiff package was used to test for a between-group difference in survival probability and to calculate a p value.

3.2.2 Generation of murine MN1-driven ldMBM leukemia cells

Bone marrow cells were isolated from tibia and femur of WT C57/BL6 mice followed by lineage-depletion using Lineage Cell Depletion Kit. Retroviral pSF91-MN1 vector (containing human leukemia-associated oncogene MN1 co-expressing green fluorescent protein (GFP) (Heuser et al., 2007)) was transfected into the Platinum-E (Plat-E) retroviral packaging cell line (purchased from Cell Biolabs, Inc; CA, USA) using TurboFect Transfection Reagents. 16h after transfection, medium was changed and retroviral supernatants were collected at 24h and 48h afterwards. Lineage-depleted mouse bone marrow (ldMBM) cells were transduced with MN1-GFP retroviruses in 2 consequential days. 3 days after the first transduction, GFP⁺ cells were sorted using BD FACSAria III.

3.2.3 Generation of stable p62 knockout in human AML cell lines by CRISPR/Cas9-based genome editing system

Knockout of p62 in human AML cell lines was performed using CRISPR/Cas9 library consisting of three guide RNAs (gRNAs) targeting

human p62 #1 (5'-TGGCTCCGGAAGGTGAAACA-3'), #2 (5'-CATTGAAGTTGATATCGATG-3') and #3 (5'-AGCCATCGCAGATCACATTG-3') sub-cloned into the pLentiCRISPR v2 GFP-Puro. Three different non-targeting control gRNAs were cloned into the pLentiCRISPR v2 Puro vector. HEK293T cells were co-transfected with lentiviral pooled library vectors and the packaging plasmids psPAX2 and pMD2.G using Polyethylenimine (PEI). 16h after transfection, medium was changed and supernatants enriched in viruses were collected 72h afterwards.

Human AML cell lines THP1, U937, Molm13 and NB4 were transduced with either CRISPR/Cas9 pooled library targeting p62 or non-targeting control lentiviral particles and selected for positive clones using puromycin (concentration 1µg/ml in THP1 and 400ng/ml for other cell lines) for 3 days.

3.2.4 Generation of stable p62 knockdown in murine MN1-driven ldMBM leukemia cells by lentiviral shRNA transduction system

Knockdown of p62 in murine MN1-driven ldMBM leukemia cells was performed by shRNA (TRCN0000238133, Sigma-Aldrich, sequence: 5'-CCGGTAGTACAACTGCTAGTTATTTCTCGAGAAATAACTAGCAGTTGTAC TATTTTTG-3') that targets the 3' UTR of the murine endogenous p62. Non-targeting shRNA (SHC002, Sigma-Aldrich, sequence: 5'-CCGGCAACAAGATGAAGAGCACCAACTC-3') was used as control.

shRNAs were cloned into lentiviral vector pLKO.1-puro and co-transfected with the packaging vectors pMD2.G and pCMV Δ8.91 into HEK293T cells using TurboFect Transfection Reagents. 16h after transfection, medium was changed and supernatants were collected at 24h and 48h afterwards. MN1-driven ldMBM leukemia cells were transduced with shp62 and shCtrl lentiviruses and selected for positive clones using 10µg/ml puromycin for 3 days.

In the rescue experiments, different p62 constructs (p62 wildtype, p62 ΔLIR (deletion of 11 amino acids S334 – S344) and p62 K7A/D69A) were sub-

cloned into the lentiviral vector SBW (expressed TagBFP) and co-transfected with the packaging vectors pMD2.G and pCMV Δ8.91 into HEK293T cells using TurboFect Transfection Reagents. Medium was changed 16h after transfection and supernatants were collected at 24h and 48h afterwards. shp62 MN1-driven ldMBM leukemia cells were subsequently transduced with different p62 constructs co-expressed TagBFP lentiviruses. shCtrl and shp62 cells were transduced with TagBFP-only lentiviruses (produced by transfection of HEK293T with SBW vector) as control and knockdown, respectively. 3 days after transduction, GFP$^+$ BFP$^+$ cells were sorted with BD FACSAria III.

3.2.5 Competitive proliferation assay

In the human AML cell lines, puromycin selected cells were co-cultured in a ratio 50% GFP$^+$ (p62) : 50% GFP$^-$ (NHT) and GFP expression was monitored daily using flow cytometry. In the murine MN1-driven ldMBM leukemia cells, MN1-GFP$^+$ cells were transduced with TagBFP cloned in lentiviral vector SBW and sorted for BFP$^+$. GFP$^+$ BFP$^-$ and GFP$^+$ BFP$^+$ cells were both transduced with lentiviral p62-shRNA (shp62) and non-targeting-shRNA (shCtrl), selected with puromycin and co-cultured crossover with a ratio 50% GFP$^+$ BFP$^-$: 50% GFP$^+$ BFP$^+$. Changes in proportion of GFP$^+$ BFP$^-$: GFP$^+$ BFP$^+$ was monitored daily using flow cytometry to determine BFP expression in sp62 and shCtrl cells.

3.2.6 Colony-forming unit assay

To analyze the colony-forming ability, cells were plated in methylcellulose Methocult GF M3534. Colonies were counted microscopically at day 10 of culture. Absolute cell numbers were determined by counting using Trypan Blue after washing out all cells from the plates.

3.2.7 Generation of murine leukemia model

Lineage-depleted mouse bone marrow cells (ldMBM) transduced with leukemia-associated oncogene MN1 co-expressing GFP from WT and p62$^{-/-}$ mice were generated as described above. 3 days after transduction, 10^5 MN1-GFP$^+$ WT or p62$^{-/-}$ cells were injected together with 10^5 supporting WT mononuclear cells into the tail vein of lethally irradiated (11Gy) WT recipient mice. Moribund mice were sacrificed. At time of death, body weight, spleen and liver weight were recorded. Differential analysis of peripheral blood was examined by Animal Blood Counter. Bone marrow and spleen cells were isolated, analyzed by flow cytometry and morphologically examined by Giemsa staining. Survival analysis was performed by Kaplan-Meier curve using GraphPad Prism (GraphPad software).

3.2.8 SILAC-labeled interactome analysis

Labeling of murine p62$^{-/-}$ and WT ldMBM leukemia cells via stable isotope labeling with amino acids in cell culture (SILAC) were performed as described (Oellerich et al., 2013). Cells were expanded for 14 days in light (p62$^{-/-}$ cells), medium (WT cells) and heavy (WT cells treated with 100nM Baf for 3h) isotope-containing IMDM for SILAC medium supplemented with 10% dialyzed FBS, 1% penicillin/streptomycin and following cytokines: 50ng/ml mSCF, 10ng/ml mIL-3 and 10ng/ml mIL-6. Cells were lysed in NP40 lysis buffer containing 150nM NaCl, 50nM Tris (pH 7.5-7.8), 5mM NaF, 0.5% NP40, 1xProtease Inhibitor Cocktail and 2mM sodium orthovanadate. Cell lysates were incubated with mouse anti-SQSTM1/p62 (used for Western Blot) overnight at 4°C. All proteins that bound into p62 were co-immunoprecipitated using Protein A/G PLUS-Agarose beads. Pulldown lysates were mixed equimolar light/medium/heavy and analyzed by mass spectrometry as previously described (Oellerich et al., 2013).

3.2.9 Flow cytometry

Flow cytometry was performed using BD LSRFortessa™. For cell surface analysis, cells were washed in PBS and stained with the appropriate antibodies for 15 minutes in room temperature. Cells were washed three times with PBS and subsequently stained with apoptotic marker 7-Aminoactinomycin D (7AAD) for 5 minutes, washed two times with PBS and analyzed.

Apoptosis analysis was performed by staining with apoptotic marker APC-conjugated Annexin V and 7AAD according to manufacturer's instructions and analyzed. To measure the mitochondrial superoxide levels using flow cytometry, cells were incubated with 5µM MitoSOX™ Red mitochondrial superoxide indicator in culture medium for 10 minutes at $37^{o}C$ in the dark. Cells were then gently washed three times with PBS, resuspended in PBS and analyzed. BrdU Cell Proliferation Assay was performed by flow cytometry using BrdU Flow Kit according to manufacturer's instructions.

3.2.10 Measurement of oxygen consumption rate

Mitochondrial respiration was measured by the oxygen consumption rate (OCR) of cells in real time by the fully integrated 96-well Seahorse XF96 Extracellular Flux Analyzer using the XF Cell Mito Stress Test Kit. 0.5×10^{6} cells were seeded in growth medium at $37^{o}C$ in XF96 Polystyrene Cell Culture Microplate for 3 hours. Afterwards, cells were washed twice with basal DMEM and kept in culture at $37^{o}C$ for an additional 1h without CO_2 in the stress assay medium as described by the manufacturer. OCR was measured in the presence of 20µM oligomycin, 50µM FCCP, antimycine and rotenone each 20µM (all reagents were included in kit).

3.2.11 Western blotting

Cell pellets were lysed in NP40 lysis buffer on ice for 30 minutes. Cell lysates were clarified by centrifugation at 15000rpm for 10 minutes at $4^{o}C$. Soluble

protein lysates were subjected to SDS polyacrylamide gel electrophoresis (PAGE) using XCell SureLock™ Mini-Cell Electrophoresis System, which was run in 1x MES SDS Running buffer. Gel was in turn transferred to nitrocellulose membrane using transfer buffer containing 25mM Tris, 192mM glycine and 10% methanol. Membrane was blocked 1h with 5% milk dissolved in PBST (PBS and 0.1% Tween® 20) solution at room temperature (RT). After washing with PBST, membrane was probed with primary antibodies which were diluted in 5% BSA dissolved in PBST solution overnight at 4°C. After 3 times 10 minutes washing with PBST solution, membrane was probed with secondary antibody conjugated with horseradish peroxidase (HRP) for 1h at RT. Afterwards, membrane was washed 3 times 10 minutes with PBST solution, developed using SuperSignal™ West Femto and visualized using Odyssey FC imaging system. Density analysis of Western Blot was performed using AlphaEase Software (Alpha Innotech).

3.2.12 Immunofluorescent staining of MN1-driven murine leukemia cells

10^{5} cells were washed and resuspended in 100µl PBS supplemented with 10% FCS. Cytospins were performed to attach suspension cells onto the cover slip. Cells were fixed in 4% PFA washed with PBS and permeabilized with 0.5% Triton X. After washing with PBS, cells were treated with Image-IT FX Signal Enhancer, followed by washing with PBS and blocked in BlockAid solution. Subsequently, blocking solution was removed and primary antibodies diluted in blocking solution were applied directly on cells for overnight incubation at 4°C. After washing with PBS, secondary antibodies diluted in blocking solution were applied for 1h at RT in darkness. Cells were then washed with PBS and cell nuclei were counterstained with 300nM DAPI. After washing with PBS, cells were mounted in Prolong Diamond Antifade Mountant and dried overnight at 4°C. Images were captured using a confocal microscope Leica TCS SP5 II (63x oil immersion objective) and LAS AF Software (Leica Microsystems).

3.2.13 Mitophagy quantification by co-localization of LC3 puncta and Tom20

Mitophagy quantification was performed as described by Allen et al. (Allen et al., 2013). Briefly, co-localization percentage was determined using ImageJ software as total LC3 puncta co-localized with Tom20 signal per total LC3 puncta detected after treatment with DFP. Only cells that contain at least 3 LC3 puncta were counted.

3.2.14 Vacuole analysis

10^5 bone marrow cells were spinoculated and stained with Giemsa. The number of cells with vacuoles within one slide was counted using the ImageJ software. Correlation analysis was performed by Pearson's correlation using the GraphPad Prism 5 (GraphPad software).

3.2.15 Total RNA isolation

Total RNA was isolated using TRI Reagent® according to the manufacturer's protocol. RNA concentration was measured using NanoDrop 2000c Spectrophotometer.

3.2.16 Relative mRNA expression analysis using quantitative real-time PCR

The mRNA expression was determined using real-time PCR. Total mRNA was isolated as described in 2.2.15 and reverse transcribed in complementary DNA (cDNA) using RevertAid H Minus Reverse Transcriptase according to the manufacturer's protocol. cDNA was amplified using SYBR® Green JumpStart™ Taq ReadyMix according to the manufacturer's instructions on the DNA Engine Opticon 2 Real-Time Cycler. MJ Opticon Monitor Analysis Software (Bio-Rad) was used for the quantification of SYBR Green fluorescent signal and the threshold cycle (Ct). Relative mRNA expression was calculated using the $2^{-\Delta\Delta Ct}$ method (Rao et

al., 2013), ß-actin served as a reference gene. Primers used for qPCR were: p62 (forward: 5'-AGAATGTGGGGGAGAGTGTG-3', reverse: 5'-TTTCTGGGGTAGTGGGTGTC-3'), ß-actin (forward: 5'-ACCCTAAGGCCAACCGTGAAA-3', reverse: 5'-CAGAGGCATACAGGGACAGCA-3'). The real-time PCR program was performed using the following cycling parameters: initial denaturation at $95^{o}C$ for 10 minutes followed by 38 cycles of denaturation at $95^{o}C$ for 15s, annealing at $58^{o}C$ for 30s and extension at $72^{o}C$ for 10s.

3.2.17 Statistical analysis

Data are shown in mean value ± standard error of the mean (SEM). All statistical tests and diagrams unless stated otherwise were performed in GraphPad Prism 5 software. Normally distributed groups were compared using 2-tailed Student t test with $p \leq 0.05$ considered as statistically significant. Correlation analysis was performed using Pearson´s correlation.

4. Results

4.1 High p62 levels in AML blasts are associated with poor survival

Previous reports have demonstrated that high p62 expression correlates with poor survival and prognosis in different cancer types (Iwadate et al., 2014; Iwadate et al., 2015; Wang et al., 2015). Therefore, it was hypothesized that p62 may also have a prognostic role in AML and examined its relevance on clinical outcome in AML patients. Thus, p62 expression values from RNA sequencing data and survival data from the TCGA LAML data set (Ley et al., 2013) containing 173 adult patients with *de novo* AML were analyzed. Kaplan-Meier survival curves of AML patients were stratified by low (first quartile) and high (fourth quartile) p62 gene expression. High p62 expression was significantly associated with poor overall survival of adult patients with *de novo* AML (Figure 5).
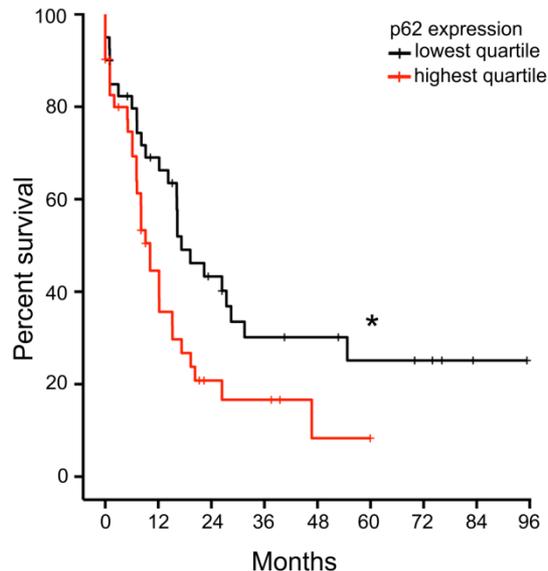
Figure 5. Correlation of p62 expression and survival of AML patients. Kaplan-Meier survival curves of adult AML patients were stratified by lowest (red) and highest (black) p62 gene expression (n = 40 in lowest quartile, n = 41 in highest quartile, p = 0.026), which was analyzed from RNA sequencing data and survival data from the TCGA LAML data set containing 173 adult patients with *de novo* AML (ns: not significant; * $p \leq 0.05$; ** $p \leq 0.01$; *** $p \leq 0.001$).

4.2 Loss of p62 impairs cell growth of human and murine AML cell lines

4.2.1 CRISPR/Cas9-based knockout of p62 diminishes cell growth in human AML cell lines

To address the functional role of p62 in human AML cell growth, CRISPR/Cas9-based knockout of p62 was performed in four different human AML cell lines THP1, U937, Molm13 and NB4. Although p62 expression levels were different across the cell lines, efficient knockout of p62 has been acquired as shown by immunoblotting. Almost no p62 expression was observed in THP1, Molm13 and NB4 cells and only a little amount of p62 protein level remaining in U937 cell (Figure 6A).
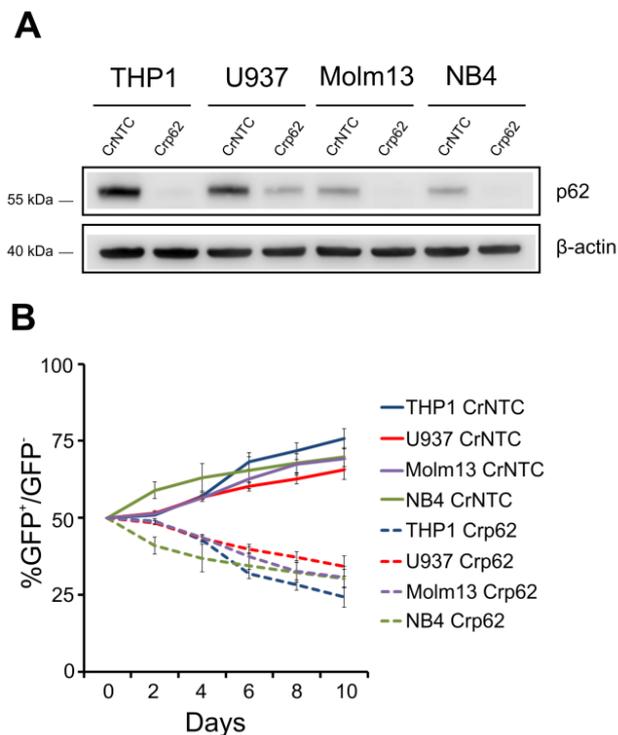
Figure 6. CRISPR/Cas9-based knockout of p62 in human AML cell lines. (A) Western blot analysis of p62 expression in CRISPR/Cas9 targeting human p62 (Crp62) and non-targeting control (CrNTC) in human AML cell lines THP1, U937, Molm13, NB4. β-actin served as loading control. (B) Competitive cell growth of CRISPR/Cas9 targeted human p62 (Crp62, GFP$^+$) and human non-targeting control (CrNTC, GFP$^-$) in human AML cell lines THP1, U937, NB4 and Molm13 measured by flow cytometry on indicated days (pooled data from three independent experiments). Values are mean ± SEM.

A competitive proliferation assay by flow cytometry has been applied to monitor the cell growth of p62 knockout cells co-expressing GFP (Crp62,

GFP$^+$) and control cells, which were transduced with non-targeting control CRIPSR-Cas9 and did not express GFP (CrNTC, GFP$^-$). As a result, knockout of p62 significantly decreased proliferation in all tested cell lines. Interestingly, reduction of cell proliferation did not only correlate with knockout efficiency of p62 but also with its basal expression level. Accordingly, the weakest effect on cell growth was detected in U937 cells, which displayed high p62 expression level but lowest knockout efficiency (drop from 50% to 34% after 10 days) (Figure 6B). In contrast, strongest reduction of cell growth was detected in THP1 cells (drop from 50% to 24% after 10 days), which also had the highest p62 expression level and knockout efficiency among all four cell lines.

In summary, these data provide a first evidence that p62 plays an essential role in leukemia cell growth.

4.2.2 Knockdown of p62 impairs proliferation and colony-forming ability in MN1-driven ldMBM leukemia cells

For further analysis, a murine leukemia cell line was generated to investigate the function of p62 in AML development and maintenance. Therefore, lineage-depleted mouse bone marrow (ldMBM) cells were transduced with the human leukemia oncogene MN1, which is known to induce AML in mice (Heuser et al., 2007). MN1-driven leukemia cells were generated to co-express the green fluorescent protein (GFP) as a selective marker. Hence, to perform the competitive proliferation assay as described above (3.2.1), an additional blue fluorescent protein (BFP) has been transduced into a subset of GFP-MN1 cells. Subsequently, GFP and BFP-MN1-driven ldMBM leukemia cells were further transduced with short-hairpin RNA (shRNA) against mouse p62 (shp62) or non-targeting control (shCtrl). After confirming efficient knockdown of p62 by Western Blot (Figure 7A) in both cell populations, competitive proliferation assay measured by flow cytometry has been applied to monitor the growth difference under p62 deficiency. Consistent with findings in human AML cell lines (Figure 6B), p62 knockdown led to inhibition of cell growth in MN1-driven ldMBM leukemia cells compared

to control cells (Figure 7B). In addition, the delayed proliferation of shp62 MN1-driven ldMBM leukemia cells was confirmed by cell expansion analysis (Figure 7C).
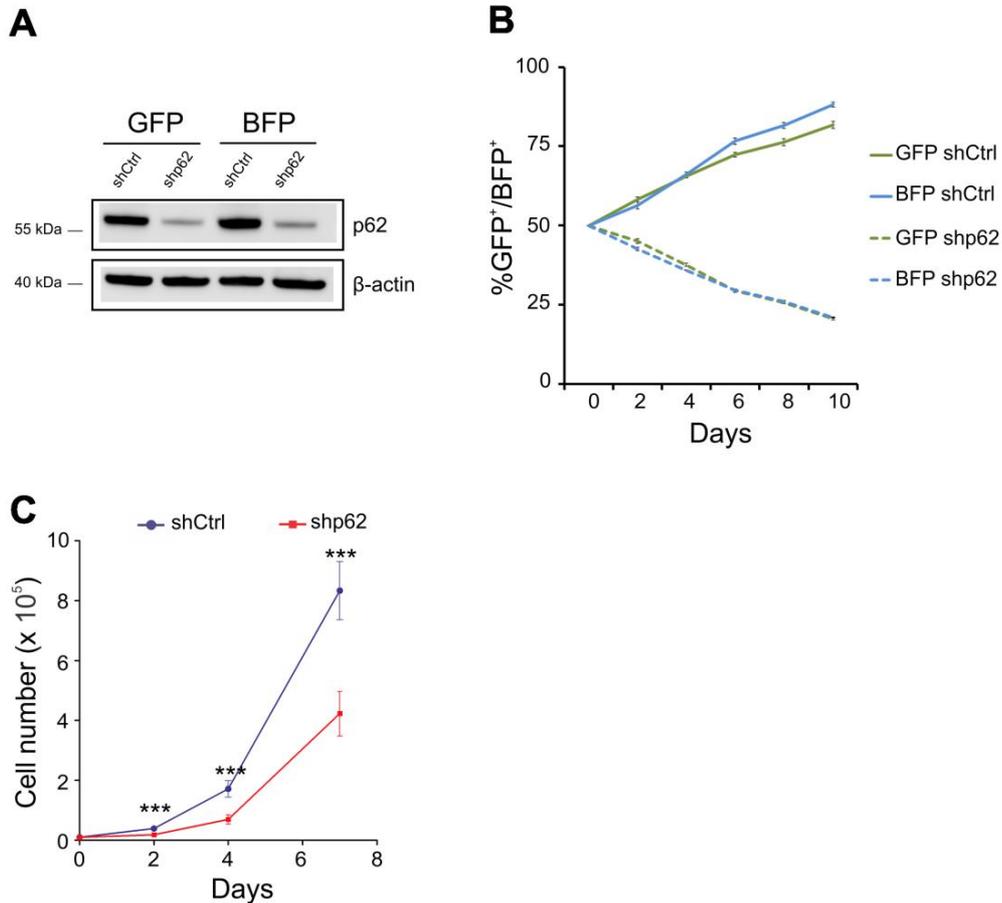
Figure 7. Knockdown of p62 using shRNA in MN1-driven ldMBM leukemia cells. (A) Western blot analysis of p62 expression in shRNA against murine p62 (shp62) or non-targeting control (shCtrl) in GFP$^+$ BFP$^-$ (GFP) and GFP$^+$ BFP$^+$ (BFP) MN1-driven ldMBM leukemia cells. β-actin served as loading control. (B) Competitive cell growth of shRNA knockdown targeting murine p62 (shp62) and non-targeting control (shCtrl) in GFP$^+$ BFP$^-$ (GFP) and GFP$^+$ BFP$^+$ (BFP) MN1-driven ldMBM leukemia cells measured by flow cytometry on indicated days (pooled data from three independent experiments). (C) Expansion analysis of p62 knockdown and control MN1-driven ldMBM leukemia cells was performed by seeding 10^4 cells and counting live cells using Trypan Blue at the indicated time points (n = 5 in triplicate). Values are mean ± SEM (ns: not significant; * p ≤ 0.05; ** p ≤ 0.01; *** p ≤ 0.001).

The ability to form colonies from a single cell indicates the self-renewal capacity of leukemia cells (Dicke et al., 1983). Hence, the functional role of p62 was determined in colony-forming ability of MN1-driven ldMBM leukemia cells by plating 500 cells in methylcellulose containing mIL3, mIL6 and mSCF cytokines. Importantly, most of the control cells gave rise to colonies (median = 320), while knockdown of p62 caused a significant reduction to half of the

colony numbers (median = 156) (Figure 8A) and total cell numbers (Figure 8B).
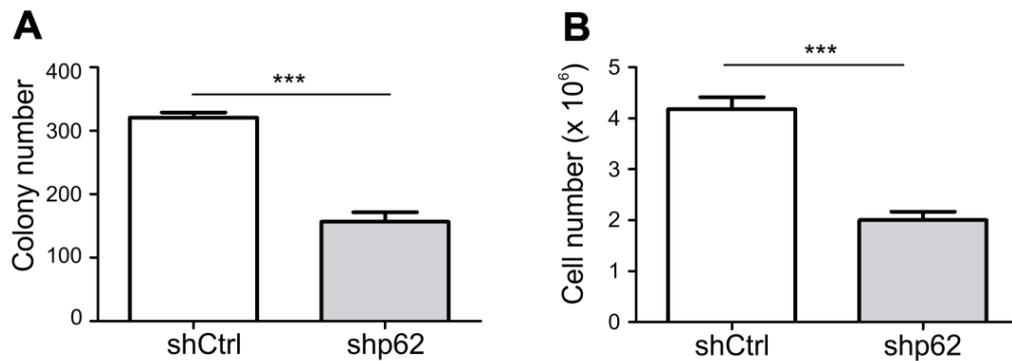
Figure 8. Colony-forming ability of p62 knockdown and control MN1-driven ldMBM leukemia cells. (A) Colony numbers and (B) cell numbers were determined in colony-forming unit assays of p62 knockdown (shp62) and control (shCtrl) MN1-driven ldMBM leukemia cells. The experiments were performed 3 times in triplicate, each with 500 cells. Values are mean ± SEM (ns: not significant; * p ≤ 0.05; ** p ≤ 0.01; *** p ≤ 0.001).

To uncover overlaying effects such as increased cell death or suppressed proliferation, apoptosis and cell cycle analyses were performed. The amount of death cells was measured by using the apoptotic marker Annexin V (early stage) and DNA dye 7AAD (late stage). Bromodeoxyuridine (BrdU) incorporation assay was used to detect DNA synthesis. Its combination with 7AAD allows to resolve cell cycle phases into G0/G1, S and G2/M phases. Notably, no difference in the apoptosis rate was detected (Figure 9A). However, cell cycle analysis showed a tendency of reduced DNA synthesis with a decreased S phase population of 31.4% upon p62 loss compared to 39% in controls (Figure 9B).
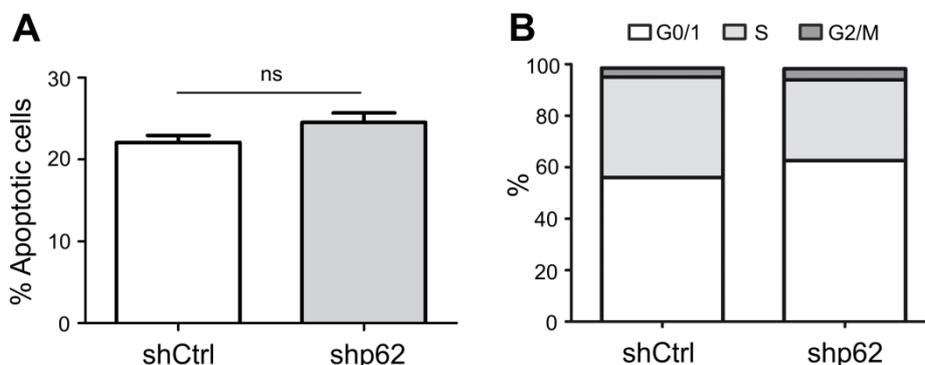
Figure 9. Apoptosis and cell cycle analysis of p62 knockdown and control MN1-driven ldMBM leukemia cells. (A) Apoptosis rate was determined in p62 knockdown and control MN1-driven ldMBM leukemia cells using flow cytometric analysis with apoptotic marker Annexin V and 7AAD (n = 5 in

triplicate). (B) Cell cycle analysis of p62 knockdown and control cells was analyzed using BrdU Cell Proliferation Assay. Values are mean ± SEM (ns: not significant; * $p \leq 0.05$; ** $p \leq 0.01$; *** $p \leq 0.001$).

Thus, loss of p62 impairs leukemia cell proliferation and decreased colony growth *in vitro*.

4.3 p62 deficiency does not affect HSC function, but delays leukemia development and maintenance in mice

4.3.1 p62 deficiency in the hematopoietic system shows no abnormalities in mice

As a first approach, the role of p62 in normal hematopoiesis was investigated by performing detailed baseline characteristics of hematopoietic compartments in $p62^{-/-}$ mice. Peripheral blood analysis revealed equal distribution of the white blood cell (WBC), red blood cell (RBC) and platelet (PLT) blood counts from WT and $p62^{-/-}$ healthy mice (Figure 10A). Flow cytometric analysis combining cell surface markers for long-term and short-term hematopoietic stem cells (LT-HSC, ST-HSC), multipotent progenitors (MPP), common myeloid progenitors (CMP) and granulocyte macrophage progenitors (GMP) showed no significant qualitative differences in the bone marrow (Figure 10B). Interestingly, a slight decrease was detected in the Lin^- $Sca1^+$ $cKit^+$ (LSK) compartment in $p62^{-/-}$ mice.
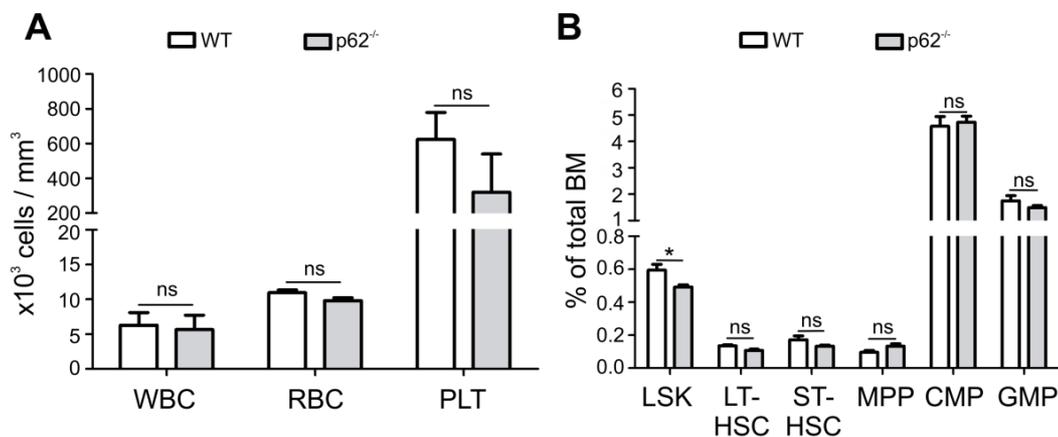
Figure 10. Compartment analysis of the bone marrow from healthy $p62^{-/-}$ and WT mice. (A) Analysis of the peripheral blood using an automated animal blood counter (WBC: white blood cell,

RBC: red blood cell, PLT: platelet). (B) Flow cytometric analysis of total bone marrow. LSK: lineage⁻ Sca1⁺cKit⁺, LT-HSC (long-term HSC): LSK Flt3⁻CD34⁻, ST-HSC (short-term HSC): LSK Flt3⁻CD34⁺, MPP (multipotent progenitors): LSK Flt3⁺CD34⁺, CMP (common myeloid progenitor): LSK CD16/32⁻ CD34⁺, GMP (granulocyte macrophage progenitor): LSK CD16/32⁺CD34⁺. n = 4 mice in each group. Values are mean ± SEM (ns: not significant; * $p \leq 0.05$; ** $p \leq 0.01$; *** $p \leq 0.001$).

The ability to form discrete colonies in semi-solid, methylcellulose-based medium supplemented with cytokines is a common feature of functional HSCs (Coulombel, 2004). Therefore, colony forming assay was performed with 2000 lineage-depleted bone marrow cells from p62⁻/⁻ and WT mice. As a result, equal colony numbers (Figure 11A) and cell numbers (Figure 11B) were observed in both groups, indicating no influence of p62 in colony-forming ability and re-plating efficiency of HSCs.
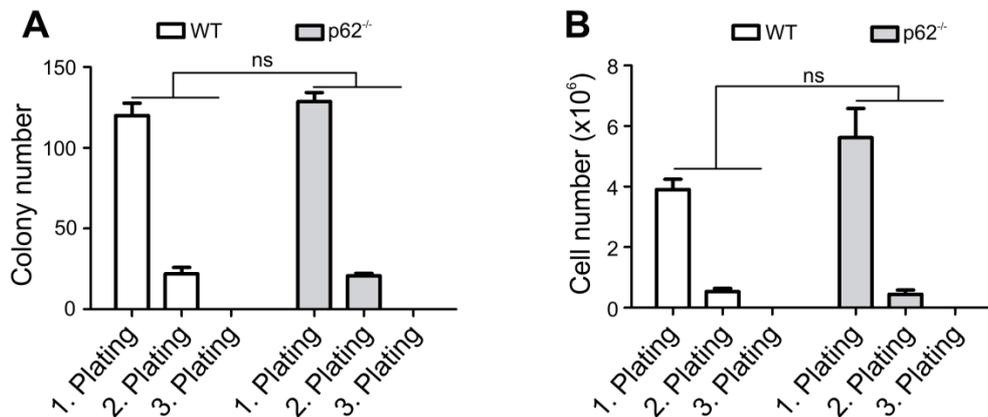
Figure 11. Functional analysis of p62⁻/⁻ and WT normal hematopoiesis. (A) Colony numbers and (B) cell numbers were determined in serial colony re-plating assay of 2000 lineage⁻ bone morrow cells derived from WT and p62⁻/⁻ mice (n = 4 mice in each group). Values are mean ± SEM (ns: not significant; * $p \leq 0.05$; ** $p \leq 0.01$; *** $p \leq 0.001$).

Taken together, p62 loss did not cause any severe alteration in the phenotype and function of normal hematopoiesis.

4.3.2 Loss of p62 delays leukemia development

As a second approach, we asked whether p62 has a role under oncogenic stress. To investigate the importance of p62 in myeloid transformation and leukemia development, a murine AML model was used. Equal numbers of GFP⁺ MN1-expressing WT or p62⁻/⁻ ldMBM cells were injected into lethally

irradiated recipient mice (Figure 12A). As expected, all mice developed a fatal myeloid leukemia. Importantly, in terms of disease progression, p62^{-/-} mice displayed a significantly longer survival (median = 38 days; range 31-47 days) than WT animals (median = 32 days; range 31-33 days) (Figure 12B).
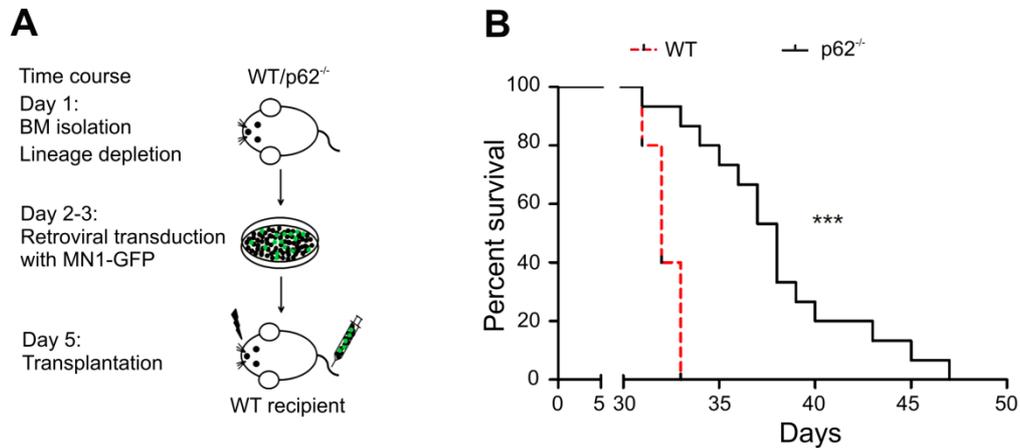
Figure 12. Transplantation of WT and p62^{-/-} MN1-driven ldMBM leukemia cells. (A) Schematic overview of the transplantation procedure. ldMBM cells from WT and p62^{-/-} donor mice were retrovirally transduced with the leukemia-associated oncogene MN1 co-expressing GFP. 10^5 MN1-GFP^{+} cells were injected into lethally irradiated (11Gy) WT recipient mice. (B) Kaplan-Meier curves represents survival of WT (n = 10) and p62^{-/-} (n = 15) MN1 leukemic mice (ns: not significant; * $p \leq 0.05$; ** $p \leq 0.01$; *** $p \leq 0.001$).

4.3.3 p62 deficient leukemia displays a more immature and vacuolated phenotype

Pathophysiological analysis of all moribund mice showed splenomegaly; however, spleen weight did not differ between the two groups (Figure 13A and 13B). Peripheral blood analyses at time of death showed increased WBC counts and decreased RBC counts in p62^{-/-} leukemic mice (Figure 13C), although bone marrow cellularity, assessed by total number of cells, were the same in both groups (WT: median = $41.2 \pm 12.2 \times 10^6$ vs p62^{-/-}: median = $42.4 \pm 8.8 \times 10^6$). Flow cytometric analysis displayed increased lineage^{-} (Lin^{-}), Lin[-]cKit^{+} and decreased CD11b^{+} populations in p62^{-/-} mice, suggesting a more immature phenotype (Figure 13D).
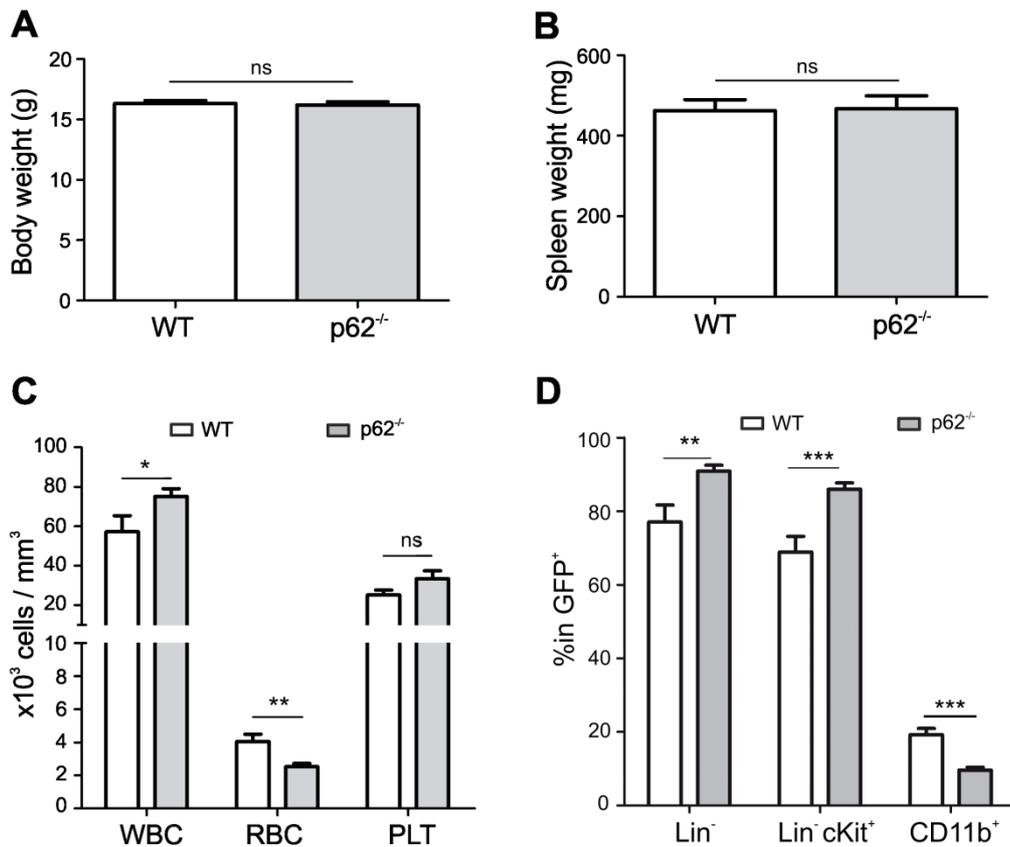
Figure 13. Characterization of WT and p62$^{-/-}$ leukemic mice. (A) Body weight and (B) spleen weight from sick mice was determined at time of death (n = 8 in WT and n = 14 in p62$^{-/-}$ mice). (C) Analysis of peripheral blood using an automated animal blood counter at time of death (WBC = white blood cell, RBC = red blood cell, PLT = platelet count). (D) Flow cytometric analysis of Lin$^-$, Lin$^-$cKit$^+$ and CD11b$^+$ (n = 8 in WT and n = 14 in p62$^{-/-}$ group) at time of death. Values are mean ± SEM (ns: not significant; * p ≤ 0.05; ** p ≤ 0.01; *** p ≤ 0.001).

This was consistent with morphological assessment of bone marrow cells from leukemic mice. Bone marrow from p62$^{-/-}$ leukemic mice was infiltrated dominantly by blasts characterized by large round nucleus with fine chromatin and scant cytoplasm. Conversely, more donut-shaped differentiated granulocytes were observed in the bone marrow of WT leukemic mice as shown by representative microscopic images (Figure 14A). In addition, vacuolization of blasts was detected, which was obviously increased in p62$^{-/-}$ leukemic mice (Figure 14B). Interestingly, there was a positive correlation between the percentage of vacuolated cells and survival time of mice (Figure 14C). Although vacuolization of cells is known to be accompanied with cell death in mammalian cells (Shubin et al., 2016), the

origin and role of these vacuoles in p62-deficient leukemia still remain an open question.
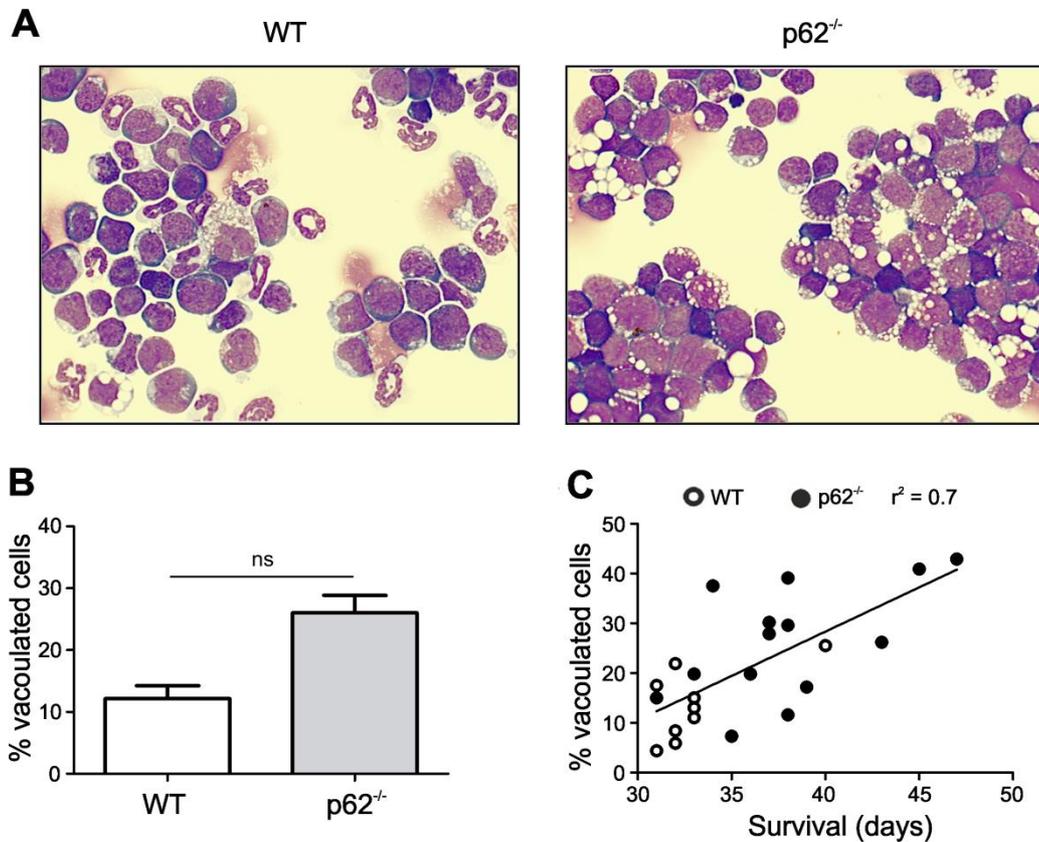
Figure 14. Morphological assessment of WT and p62$^{-/-}$ leukemic bone marrow. (A) Representative microscopic depiction of WT and p62$^{-/-}$ bone marrow from leukemic mice (arrow head: leukemic blast, arrow: differentiated granulocyte, ∗: vacuolated cell). (B) Quantitative assessment of vacuolated cells in WT and p62$^{-/-}$ leukemic mice (n = 8 in WT and n = 14 in p62$^{-/-}$). (C) Correlation between the percentage of vacuolated cells and the survival of mice. Values are mean ± SEM (ns: not significant; * p ≤ 0.05; ** p ≤ 0.01; *** p ≤ 0.001).

4.3.4 Colony-forming ability is impaired in p62 deficient leukemia cells

To further characterize the importance of p62 in leukemia progression, functional analyses from the *in vivo* experiment were performed. *Ex vivo* colony-forming assays displayed lower colony numbers and cell numbers (Figure 15A and 15B) in p62$^{-/-}$ leukemic mice. Flow cytometric analysis using apoptotic markers Annexin V and 7AAD revealed no difference in the rate of apoptotic cells between both groups (Figure 15C).
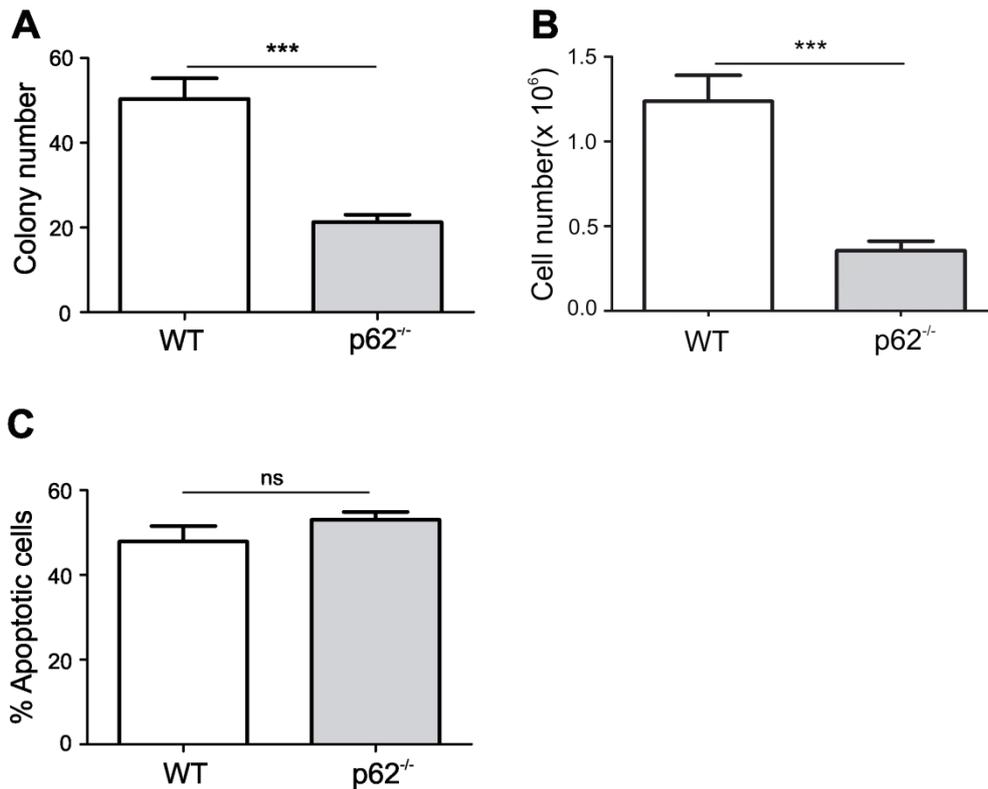
Figure 15. Colony-forming ability and apoptosis rate of WT and p62$^{-/-}$ MN1-driven IdMBM leukemia cells from sick mice. (A) Colony numbers and (B) cell numbers were determined in colony-forming unit assays of p62$^{-/-}$ and WT MN1-driven IdMBM leukemia cells isolated from the bone marrow of sick mice at time of death (n = 8 in WT and n = 14 in p62$^{-/-}$ group). Each experiment was performed in triplicate with 500 cells. (C) Apoptosis rate was measured in WT and p62$^{-/-}$ cells using flow cytometric analysis of apoptotic marker Annexin V and 7AAD (n = 8 in WT and n = 14 in p62$^{-/-}$). Values are mean ± SEM (ns: not significant; * $p \leq 0.05$; ** $p \leq 0.01$; *** $p \leq 0.001$).

Taken together, consistent with the *in vitro* data (as shown in Figure 7, 8 and 9), impaired proliferation was observed in p62$^{-/-}$ leukemic cells which was not caused by increased apoptosis rate.

4.3.5 p62 deficiency delays leukemia maintenance

To characterize the effect of p62 loss in leukemia maintenance, secondary re-transplantation of primary MN1-driven leukemia cells derived from sick mice into WT recipient animals was performed (Figure 16A). Similar to the primary transplantation, leukemia progression was significantly diminished in p62$^{-/-}$ mice (median = 41 days; range 31-51 days) compared to WT mice (median = 31 days, range 26-41 days) (Figure 16B).
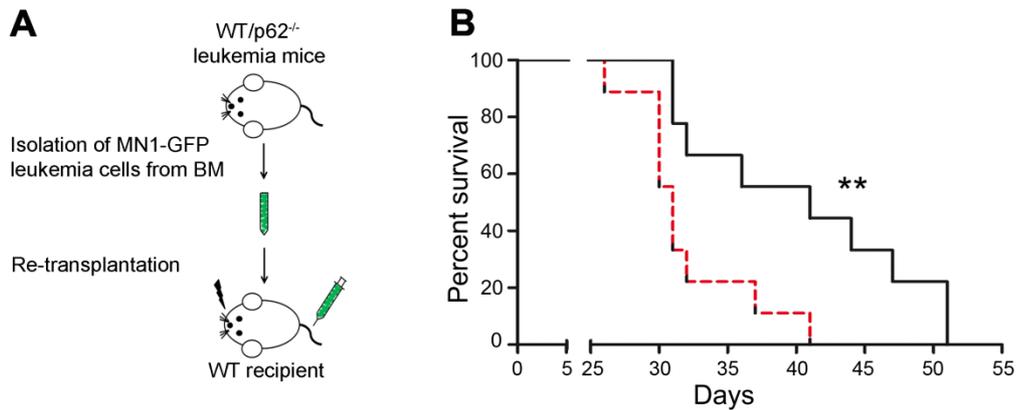
Figure 16. Secondary re-transplantation of WT and p62$^{-/-}$ MN1-driven ldMBM leukemia cells. (A) Schematic overview of the re-transplantation procedure. 10^4 primary GFP-MN1-driven ldMBM cells from WT and p62$^{-/-}$ leukemia mice were injected into sub-lethally irradiated (5.5Gy) WT recipient mice. (B) Kaplan-Meier curves represents survival of secondary recipients transplanted with WT or p62$^{-/-}$ MN1 leukemic mice (n = 9 in both groups). Values are mean ± SEM (ns: not significant; * p ≤ 0.05; ** p ≤ 0.01; *** p ≤ 0.001).

Taken together, p62 is highly required for rapid MN1-driven leukemia development and maintenance.

4.4 p62 interacts with mitochondria in an autophagy-dependent manner in MN1 leukemia cells

To gain molecular insight into the function of p62 during myeloid transformation, stable isotope labeling with amino acids in cell culture (SILAC)-based quantitative proteomic experiments was performed to identify interaction partners of p62 in an unbiased manner (Mann, 2006). In this interactome analysis, WT MN1-driven ldMBM leukemia cells were labeled with medium (M) isotope and p62$^{-/-}$ leukemia cells, labeled with light (L) isotope, served as a negative control. In order to maximize p62 interaction with putative autophagic cargoes, WT leukemia cells, labeled with heavy (H) isotope, were treated with the lysosomal inhibitor bafilomycin A1 (Baf) (Figure 17). This experimental setup allowed separation between interaction partners (ratio H/L ≥ 1.5) and unspecific background (ratio H/L ~ 1).
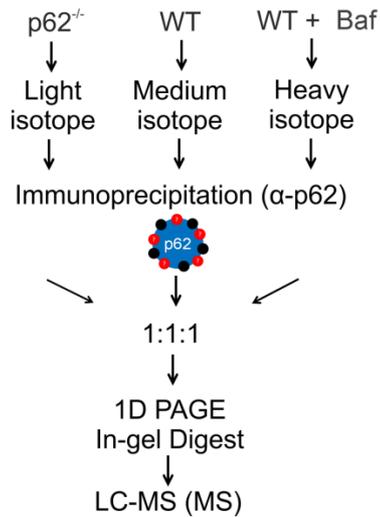
Figure 17. Schematic illustration of SILAC-interactome analysis in murine MN1-driven ldMBM leukemia cells. p62^{-/-} MN1-driven ldMBM cells were cultured in light SILAC medium served as negative control. WT MN1-driven ldMBM cells were grown in medium SILAC medium and WT cells treated with Baf were labelled with heavy isotope. p62 was immunoprecipitated from cell lysates of all three conditions. Precipitated proteins were mixed in equimolar amounts followed by 1D PAGE separation and analyzed by mass spectrometry.

31 proteins were detected which were enriched in the heavy SILAC states. These included p62 as the immunoprecipitated bait protein and Keap1, a well-known p62 binding partner (Ichimura et al., 2013), confirming the reliability of the results. Importantly, 35% interaction partners were classified as mitochondrial proteins according to the Swiss-Prot database and a literature search. The detected mitochondrial proteins were localized in the mitochondrial membrane and matrix. However, localization for some of the proteins has not been determined. Other putative binding partners of p62 were found in the endoplasmic reticulum (ER), aggresomes, cytoplasma, cellular membrane and exosomes (Table 7).

Gene	Protein	Ratio M/L	Ratio H/L	Ratio H/M	Autophagy dependency
SQSTM1/P62	Sequestosome-1	5.6	37.0	6.7	+
p62 known binding partner					
KEAP1	Kelch-like ECH-associated protein 1	4.8	14.3	3.0	+

4. Results

Mitochondria					
Mitochondrial membrane					
NME2	Nucleoside diphosphate kinase B	1.6	4.7	3.0	+
SLC25A3	Phosphate carrier protein, mitochondrial	3.2	4.0	1.3	+
SLC25A5	ADP/ATP translocase 2	2.2	2.5	1.2	+
Mitochondrial matrix					
GOT2	Aspartate aminotransferase, mitochondrial	4.7	6.3	1.3	+
OAT	Ornithine aminotransferase, mitochondrial	2.7	3.0	1.1	+
MDH2	Malate dehydrogenase, mitochondrial	2.3	2.9	1.3	+
HSPE1	10 kDa heat shock protein, mitochondrial	1.4	2.0	1.4	+
Undefined mitochondrial location					
TMEM160	Transmembrane protein 160	3.3	39.9	12.2	+
TGM2	Protein-glutamine gamma-glutamyltransferase 2	1.0	3.9	4.0	+
FASN	Fatty acid synthase	1.0	2.3	2.4	+
PKM	Pyruvate kinase	1.8	2.2	1.2	+
Endoplasmic reticulum					
P4HB	Protein disulfide-isomerase	3.9	5.3	1.4	+
PDIA3	Protein disulfide-isomerase A3	4.1	4.9	1.2	+
CALR	Calreticulin	3.4	4.1	1.2	+
LRRC59	Leucine-rich repeat-containing protein 59	8.4	3.2	0.4	-
HSP90B1	Endoplasmin	1.2	2.9	2.4	+
HSPA5	78 kDa glucose-regulated protein	1.1	2.7	2.5	+
GANAB	Neutral alpha-glucosidase	1.2	2.5	2.1	+

CANX	Calnexin	0.9	2.2	2.5	+
DDOST	Dolichyl-diphosphooligosaccharide-- protein glycosyltransferase 48 kDa subunit	1.5	2.0	1.3	+
Aggresome					
EEF2	Elongation factor 2	24.1	5.4	0.2	-
Cytoplasm					
ARHGDIA	Rho GDP-dissociation inhibitor 1	1.2	3.6	2.9	+
PGAM1	Phosphoglycerate mutase 1	0.9	2.5	2.8	+
ACTR2	Actin-related protein 2	2.3	2.3	1.0	-
MIF	Macrophage migration inhibitory factor	1.5	2.1	1.4	+
HSPA4	Heat shock 70 kDa protein 4	1.1	2.0	1.8	+
Cellular membrane					
MSN	Moesin	1.0	2.5	2.4	+
Exosome					
FERMT3	Fermitin family homolog 3	4.4	3.1	0.7	-
TKT	Transketolase	1.0	2.9	3.0	+

Table 7. List of proteins co-purified with p62 in MN1-driven ldMBM leukemia cells. SILAC-based mass spectrometry was performed to identify p62 interactors in MN1-driven leukemia cells, as shown in Figure 17. Listed are all proteins that were at least 1.5 fold enriched in the H/L ratio. Localization of each co-purified protein was classified according to the Swiss-Prot database and a general literature search. Proteins with a ratio H/M > 1 were considered autophagy-dependent, as their co-purification with p62 increased after autophagy inhibition with Baf.

To determine the impact of autophagic accumulation of putative p62 interactors, the ratio H/M was calculated by dividing the ratio M/L (untreated state) by the ratio H/L (Baf-treated state). Proteins bound to p62 with a ratio H/M > 1 (dotted line in Figure 18A) were defined as autophagy-dependent. Strikingly, an enrichment of every single detected mitochondrial protein upon inhibition of autophagic degradation was found (Figure 18B). In contrast, four

non-mitochondrial interaction partners showed H/M ratio ≤ 1, indicating autophagy-independent degradation (Figure 18A, Table 7).
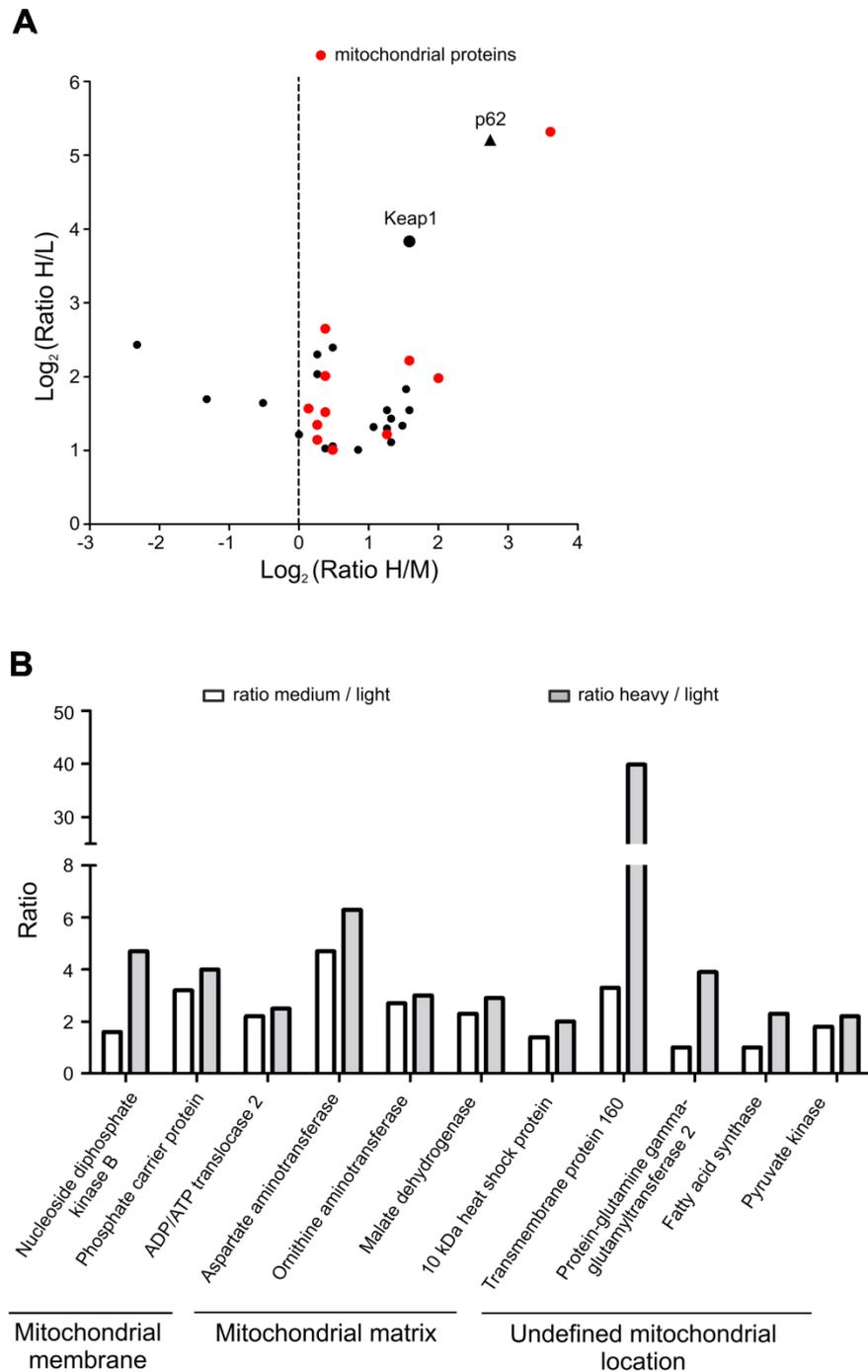
Figure 18. SILAC-interactome analysis demonstrates autophagy-dependent binding of p62 to mitochondrial proteins in MN1-driven leukemia cells. (A) Proteins with heavy/light (H/L) ratio ≥ 1.5 are plotted against their heavy/medium (H/M) ratio on a logarithmic scale. Dotted line indicates ratio H/M = 1, red dots represent mitochondrial proteins. (B) Binding ratio analysis of mitochondrial proteins under steady state condition (ratio M/L) and after treatment with Baf (ratio H/L).

Taken together, these findings strongly suggest that p62 binding to mitochondria occurs predominantly in an autophagy-dependent way.

4.5 Loss of p62 compromises mitochondrial function in leukemia cells

Given the fact that the interactome analysis revealed a strong interaction of p62 with mitochondrial proteins in MN1-driven leukemia cells (Figure 18), we wondered whether mitochondrial clearance and mitochondrial function between WT and p62$^{-/-}$ leukemia.

4.5.1 Absence of p62 causes morphological changes in the mitochondria

As it was reported that loss of p62 results in mitochondrial fragmentation in mouse embryonic fibroblasts (MEFs), neurons and astrocytes (Seibenhener et al., 2013), morphological analysis by confocal and electron microscopy was performed. Immunofluorescence staining for the mitochondrial outer membrane marker Tom20 revealed compacted mitochondrial structures in MN1-driven ldMBM leukemia cells, whereas fragmented and dispersed mitochondria were observed after knockdown of p62 (Figure 19).
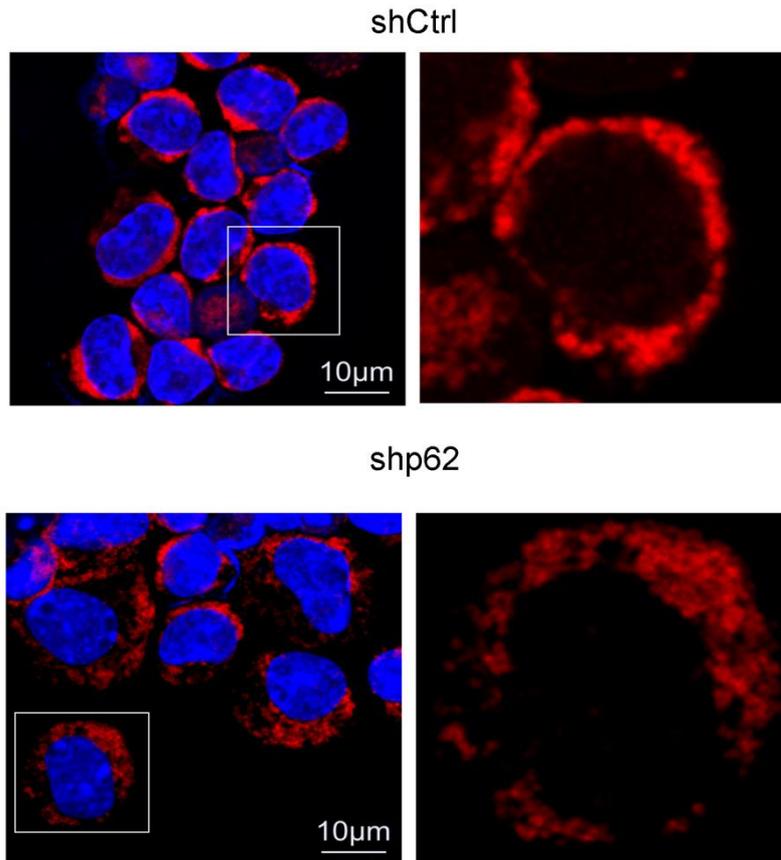
shCtrl

shp62

Figure 19. Morphological analysis of mitochondria from p62 knockdown and control MN1-driven ldMBM leukemia cells. Mitochondrial morphology analysis of control (shCtrl) and p62 knockdown (shp62) MN1-driven ldMBM leukemia cells was performed by immunofluorescence staining with the mitochondrial marker Tom20 (red). DAPI (blue) was used as a nuclear counterstain. Scale bar = 10 µm.

Electron microscopy analysis from p62 knockdown cells revealed further differences in the ultrastructure of mitochondria, as they appeared shortened and rounded with swollen cristae compared to control cells. Interestingly, p62 knockdown also affected mitochondrial biogenesis as the number of mitochondria were decreased (Figure 20).

shCtrl
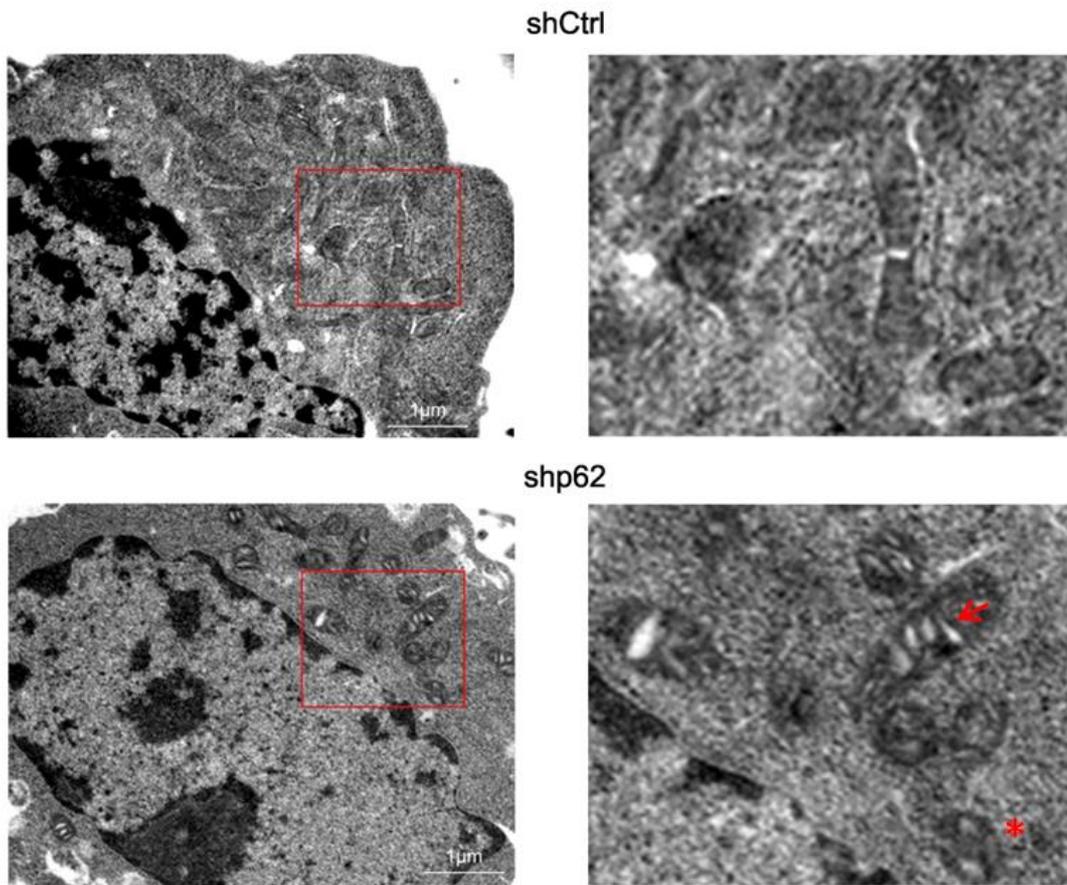
shp62

Figure 20. Electron microscopy of the mitochondria ultrastructure from p62 knockdown and control MN1-driven ldMBM leukemia cells. Morphological analysis of mitochondria by electron microscopy in WT and shp62 MN1-driven ldMBM leukemia cells (∗: rounded mitochondria, arrow: swollen mitochondrial cristae).

4.5.2 Loss of p62 causes accumulation of mitochondrial superoxide and impairs mitochondrial respiration

In a next step mitochondrial function in p62$^{-/-}$ leukemic mice was investigated. Normally, functional mitochondria scavenge the superoxide anion ($O^{2-•}$) that is generated as a by-product during the mitochondrial oxidative phosphorylation (Turrens, 2003). Therefore, detection of mitochondrial superoxide levels, the primary and most abundant reactive oxygen species (ROS) can be used as a surrogate marker for mitochondrial activity (Zorov et al., 2014). However, increased levels of mitochondrial superoxide is accompanied with severe mitochondrial damage (Wang and Klionsky, 2011). To exclude the possibility that oncogenic stress itself may increase ROS production, ROS levels in MN1 blasts of leukemic mice and their equivalent

HSC compartment (Lin⁻cKit⁺) in healthy animals were determined. In the presence of p62, MN1-mediated transformation had no influence on basal ROS levels, whereas deficiency in p62 led to significant accumulation (3-fold increase) of mitochondrial superoxide in leukemic mice, indicating severe mitochondria dysfunction (Figure 21A). Notably, normal HSCs of p62$^{-/-}$ mice tended even towards lower ROS levels than WT mice. Strikingly, increased ROS level were associated with prolonged survival during leukemia development (Figure 21B).
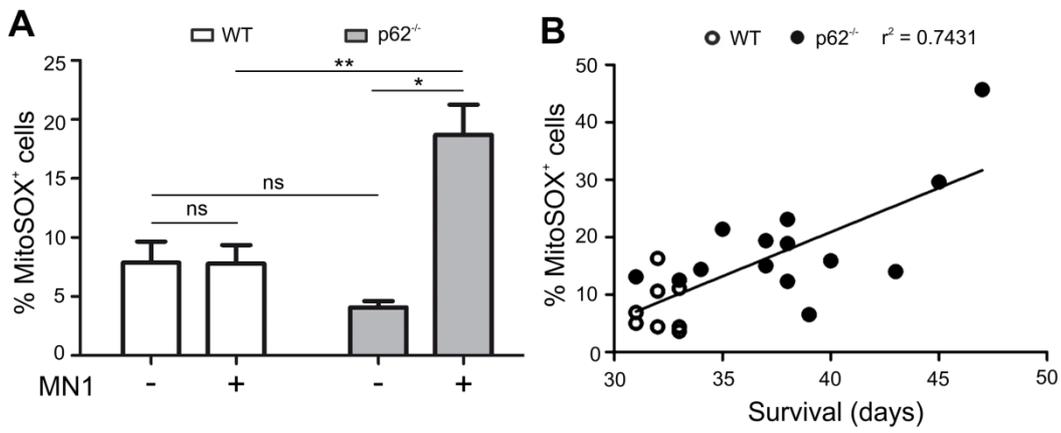
Figure 21. Mitochondrial superoxide analysis in WT and p62$^{-/-}$ MN1-driven ldMBM leukemia cells. (A) Mitochondrial superoxide levels of Lin⁻cKit⁺ HSC cells from healthy mice (n = 3 per group) and GFP⁺ Lin⁻cKit⁺ blasts from MN1 leukemic mice (n = 8 in WT and n = 14 in p62$^{-/-}$ leukemic mice) were analyzed by flow cytometry using MitoSOX. (B) Pearson's correlation was used to determine the correlation between the proportions of MitoSOX⁺ leukemic cells with the survival time of leukemic mice. Values are mean ± SEM (ns: not significant; * $p \leq 0.05$; ** $p \leq 0.01$; *** $p \leq 0.001$).

Another alternative method for quantifying mitochondrial function can be determined by measuring the mitochondrial oxygen consumption rate (OCR) (Brand and Nicholls, 2011). Importantly, mitochondria from p62$^{-/-}$ blasts displayed reduced basal and maximal respiratory capacity as well as reduced ATP production (Figure 22A and 22B), which indicates mitochondrial dysfunction.
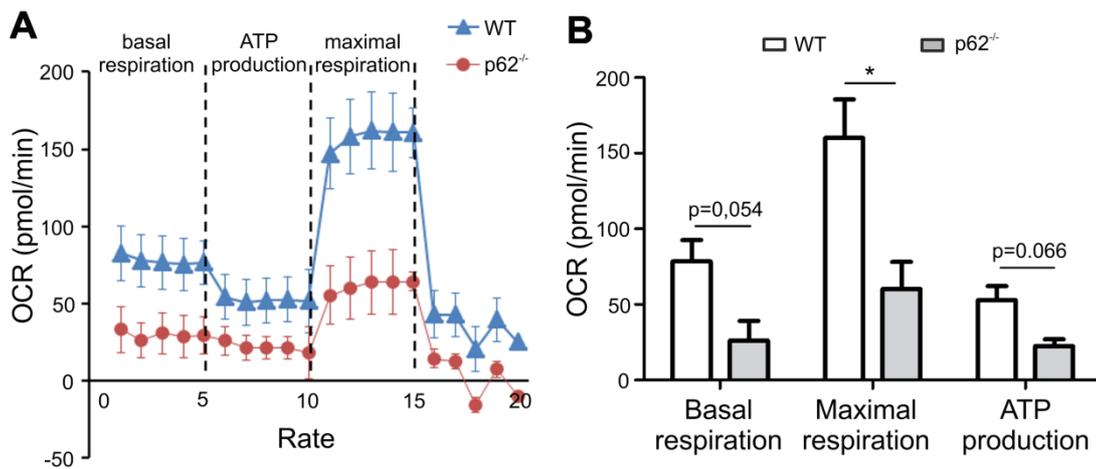
Figure 22. Mitochondrial respiration analysis in WT and p62^{-/-} MN1-driven ldMBM leukemia cells. (A) Mitochondrial respiration of leukemic blasts (n = 3 per group) was determined by measuring the oxygen consumption rate (OCR). The experiment was performed in real time by the 96-well Seahorse Bioscience Extracellular Flux Analyzer XF96. (B) The rates of basal respiration, maximal respiration and ATP production were compared between WT and p62^{-/-} group (n = 3 per group). Values are mean ± SEM (ns: not significant; * $p \leq 0.05$; ** $p \leq 0.01$; *** $p \leq 0.001$).

In summary, these data confirm a significantly compromised mitochondrial function in p62^{-/-} leukemia cells, which emphasizes the crucial role of p62 in maintaining mitochondrial homeostasis under oncogenic stress.

4.6 Loss of p62 in murine MN1-driven leukemia cells impairs mitophagy in a PINK1/Parkin-independent manner

Data generated in this thesis showed that p62 binds mitochondrial proteins in an autophagy-dependent manner (Figure 18) and loss of p62 caused accumulation of dysfunctional mitochondria (Figure 21 and 22). This led to the hypothesis that p62 may be required for mitochondrial degradation by mitophagy. To further investigate the process of mitophagy, firstly mitochondrial damage was induced and secondly efficiency of mitochondrial clearance and translocation of damaged mitochondria to the autophagosomes were detected.

4.6.1 p62 deficiency delays mitochondrial degradation

In the first approach mitochondrial degradation was examined by immunoblotting. Mitochondrial membrane depolarization after treatment with the uncoupler carbonyl cyanide m‑chlorophenylhydrazone (CCCP), frequently used to induce PINK1/Parkin-dependent mitophagy (Geisler et al., 2010), showed no degradation of the inner mitochondrial membrane protein cytochrome C oxidase subunit IV (COXIV) in MN1-driven ldMBM leukemia cells (Figure 23). This suggests that endogenous Parkin is not sufficient to induce mitophagy (Rakovic et al., 2013).
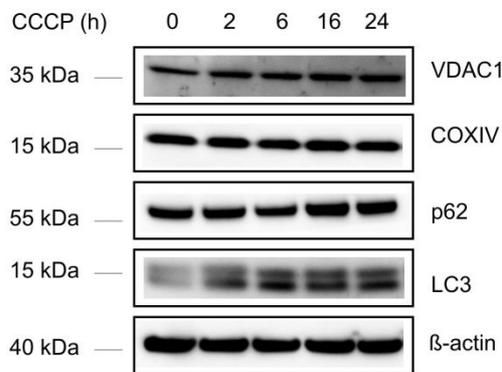
Figure 23. Assessment of PINK1/Parkin-induced mitophagy in MN1-driven ldMBM leukemia cells. MN1-driven ldMBM leukemia cells were treated with 20µM CCCP at different time points. Lysates were analyzed by Western blotting for the inner mitochondrial protein COXIV and the outer mitochondrial proteins VDAC1 and the autophagic markers p62 and LC3. β-actin served as a loading control.

To avoid Parkin overexpression, PINK1/Parkin-independent mitophagy was triggered by mitochondrial damage with the iron chelator deferiprone (DFP) (Allen et al., 2013). After DFP treatment, only 44% of COXIV protein remained in shCtrl cells, whereas 89% COXIV was still detected in shp62 cells, indicating impaired mitochondrial degradation (Figure 24A and 24B). Assessment of autophagy levels was performed by detection of the autophagosomal marker LC3. Briefly, the conversion from cytosolic LC3 (LC3-I) to autophagosome-bound LC3 form (LC-II) has been widely used to assess autophagy flux (Mizushima and Yoshimori, 2007). Of note, impaired autophagic flux was detected in shp62 cells after DFP-induced mitochondrial damage as shown by decreased LC3I conversion and LC3II turnover compared to WT cells (Figure 24A).
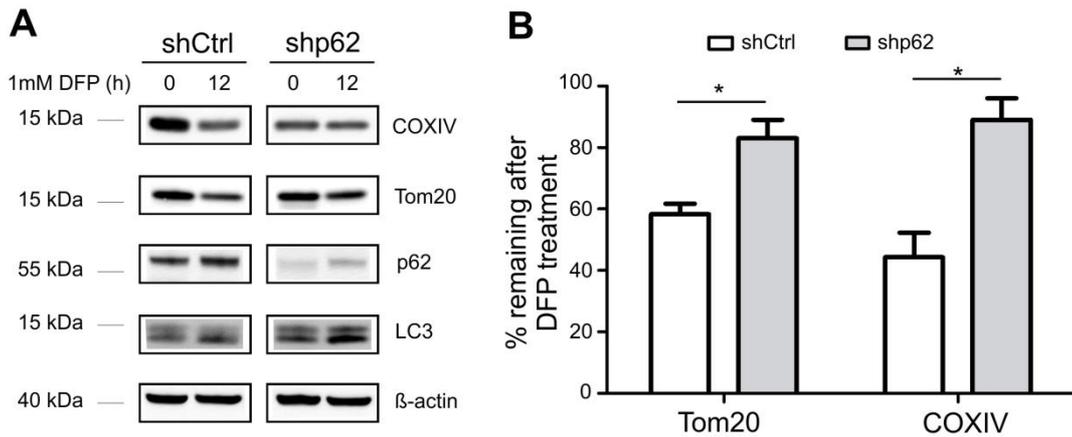
Figure 24. Assessment of PINK1/Parkin-independent mitophagy in MN1-driven ldMBM leukemia cells. (A) shCtrl and shp62 MN1-driven ldMBM leukemia cells were treated for 12h with DFP. Lysates were analyzed by Western blotting for the inner mitochondrial protein COXIV and the outer mitochondrial proteins Tom20 and the autophagic markers p62 and LC3. β-actin served as a loading control. (B) Quantification of remaining protein expression after 12h treatment with DFP of mitochondrial proteins Tom20 and COXIV compared to 0h using density analysis of Western Blots (n = 3 independent experiments). Values are mean ± SEM (ns: not significant; * p ≤ 0.05; ** p ≤ 0.01; *** p ≤ 0.001).

Interestingly, the mitochondrial degradation upon DFP treatment was accompanied by transcriptional upregulation of p62 in shCtrl cells (Figure 25A). Moreover, blocking autophagosomal degradation with the autophagosomal inhibitor BafilomycinA (Baf) inhibited the degradation of the mitochondrial inner membrane protein COXIV in shCtrl but not in shp62 cells (Figure 25B), confirming that loss of p62 prevents mitophagy.
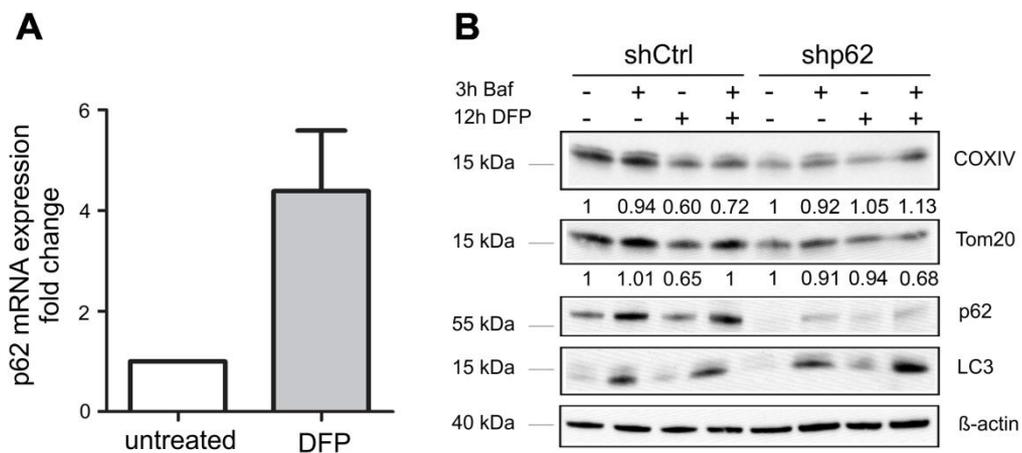
Figure 25. Mitochondrial degradation after DFP treatment depends on autophagy. (A) Quantitative real-time PCR measuring relative p62 mRNA expression in MN1-driven ldMBM leukemia cells in steady state (untreated) and after 12h DFP treatment (n = 3 independent experiments). (B) shCtrl and shp62 MN1-driven ldMBM leukemia cells underwent 3h treatment with 100nM Baf, 12h treatment with 1mM DFP or both. Lysates were analyzed by Western blotting for the inner

mitochondrial protein COXIV and the outer mitochondrial proteins Tom20 and the autophagic markers p62 and LC3. β-actin served as a loading control. Values are mean ± SEM (ns: not significant; * p ≤ 0.05; ** p ≤ 0.01; *** p ≤ 0.001).

4.6.2 p62 targets damaged mitochondria into autophagosomes

In a second approach the amount of damaged mitochondria that co-localized with autophagosomes was analyzed by confocal microscopy. For this purpose, the co-localization of the autophagic marker LC3 with the mitochondrial marker Tom20 was quantified by immunofluorescent staining (Figure 26A). After DFP treatment 72% of LC3 puncta (i.e. autophagosomes) co-localized with Tom20 (i.e. mitochondria) in shCtrl cells, whereas the co-localization rate was significantly reduced to 54% in shp62 cells (Figure 26B).
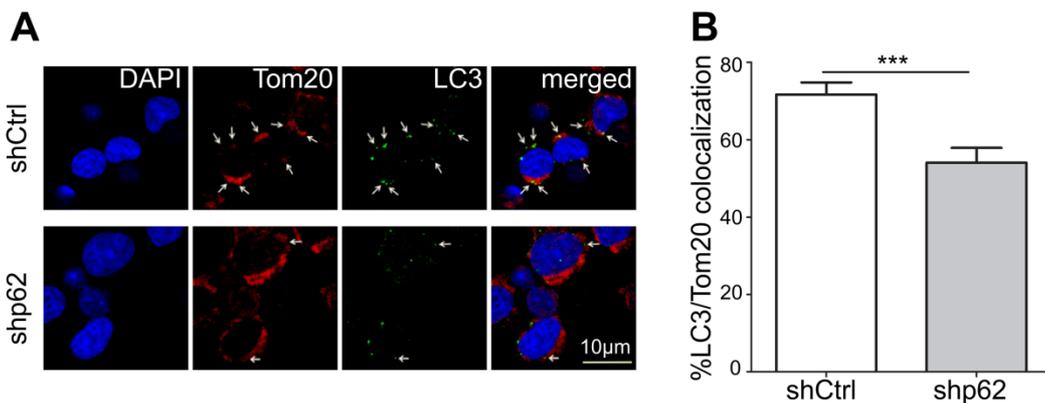
Figure 26. Confocal microscopy analysis of mitophagy after treatment with DFP in MN1-driven ldMBM leukemia cells. (A) Immunofluorescent staining of shCtrl and shp62 MN1-driven ldMBM leukemia cells after 12h treatment with DFP was performed with the mitochondrial and autophagic markers Tom20 and LC3, respectively. Arrows indicate co-localization of both markers. DAPI was used as a nuclear stain. Scale bar = 10 μm. (B) Co-localization of Tom20 and LC3 was analyzed by ImageJ (n = 50 for each group). Values are means ± SEM (ns: not significant; * p ≤ 0.05; ** p ≤ 0.01; *** p ≤ 0.001).

Taken together, p62 is required for effective targeting and degradation of damaged mitochondria by mitophagy in leukemia cells.

4.7 The autophagy-dependent function of p62 is essential for cell proliferation and efficient mitophagy

Previous data demonstrated that p62 is essential for cell proliferation (Figure 6,7 and 8) and required for efficient degradation of damaged mitochondria by mitophagy (Figure 24 and 26). Based on the fact that p62 is a multifunctional protein, we asked whether its autophagy-mediated LC3-interacting region (LIR) or its clustering-domain (PB1) are crucial for cell growth and mitophagy in MN1-driven ldMBM leukemia cells. Therefore, p62 WT and p62 mutants ΔLIR (deletion of 11 amino acids S334 – S344) and K7A/D69A of the PB1 domain (generated as previously described (Ichimura et al., 2008)) were re-expressed in shp62 cells.

4.7.1 Proliferation of MN1-driven ldMBM leukemia cells relies preferably on the autophagy-dependent domain LIR than the clustering domain PB1

Western blot analysis demonstrated that re-expression of p62 WT in shp62 cells restored endogenous protein levels, whereas expression levels of both p62 mutants were significantly elevated, suggesting their stabilization and impaired degradation (Figure 27A). Despite increased expression levels of both p62 mutants, only p62 WT was able to fully rescue cell growth (Figure 27B) and colony-forming ability (Figure 27C and 27D). Importantly, p62 ΔLIR reduced cell growth and colony-forming ability to the same extent as knockdown of p62; however, p62 K7A/D69A displayed an intermediated phenotype.
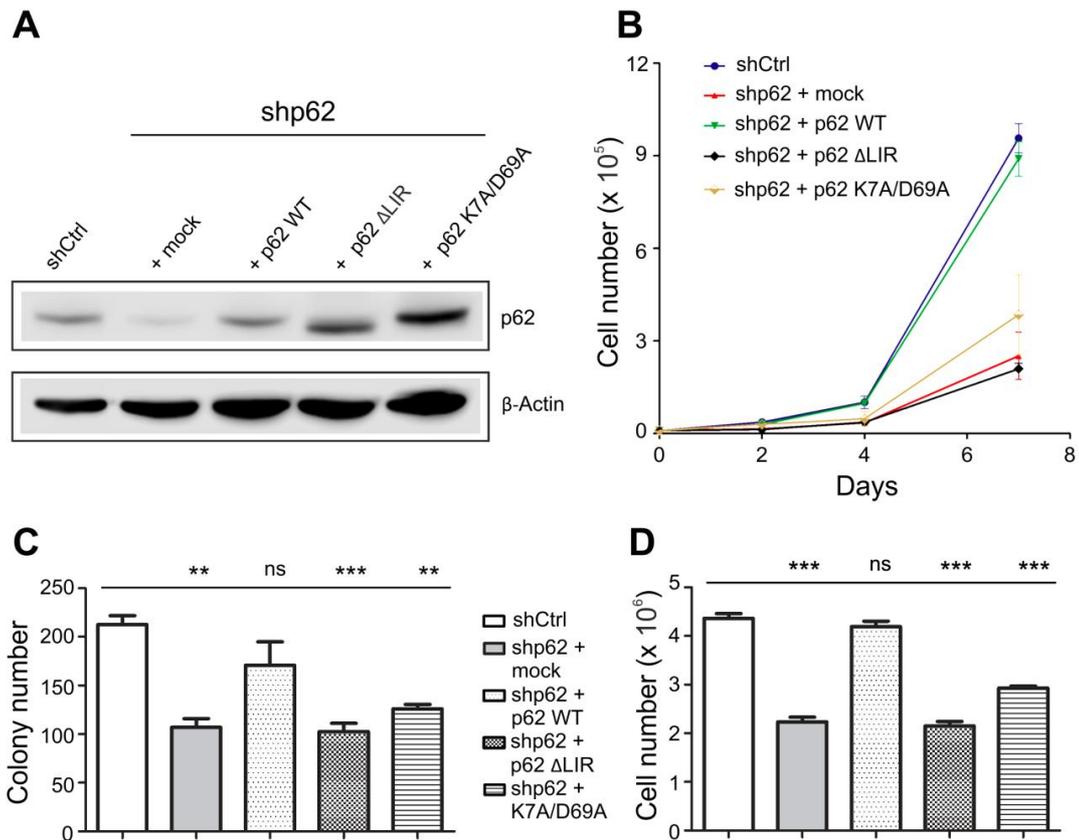
Figure 27. Proliferation analysis of rescue experiment. (A) shp62 MN1-driven ldMBM leukemia cells were transduced with empty (shp62 + mock), WT (shp62 + p62 WT) and mutant p62 constructs (LIR deletion mutant: shp62 + p62 ΔLIR, PB1 mutant: shp62 + p62 K7A/D69A). shCtrl MN1-driven ldMBM leukemia cells were transduced with empty vector (shCtrl). Expression levels of WT and p62 mutants were confirmed by immunoblotting, β-actin served as a loading control. (B) Expansion analysis of shCtrl, shp62 and p62 mutants transduced MN1-driven ldMBM leukemia cells was performed by seeding 104 cells and counting live cells using Trypan Blue at the indicated time points (n = 3 in triplicate). (C) Colony numbers and (D) cell numbers were determined in colony-forming unit assays of shCtrl, shp62 and p62 mutants transduced MN1-driven leukemia cells (n = 3 in triplicate, each with 500 cells). Values are means ± SEM (ns: not significant; * p ≤ 0.05; ** p ≤ 0.01; *** p ≤ 0.001).

4.7.2 The autophagy-dependent domain LIR but not the clustering domain PB1 is crucial for efficient mitophagy in MN1-driven ldMBM leukemia cells

Next, we confirmed that the observed proliferation differences among both p62 mutants are mitophagy-mediated. Strikingly, restoration of p62 WT and the p62-K7A/D69A mutant fully rescued the co-localization of LC3 and Tom20 upon DFP treatment from 55% back to 80% and 76%, respectively. In contrast the p62-ΔLIR mutant failed to rescue mitophagy, as co-localization remained at 57% (Figure 28A and 28B).
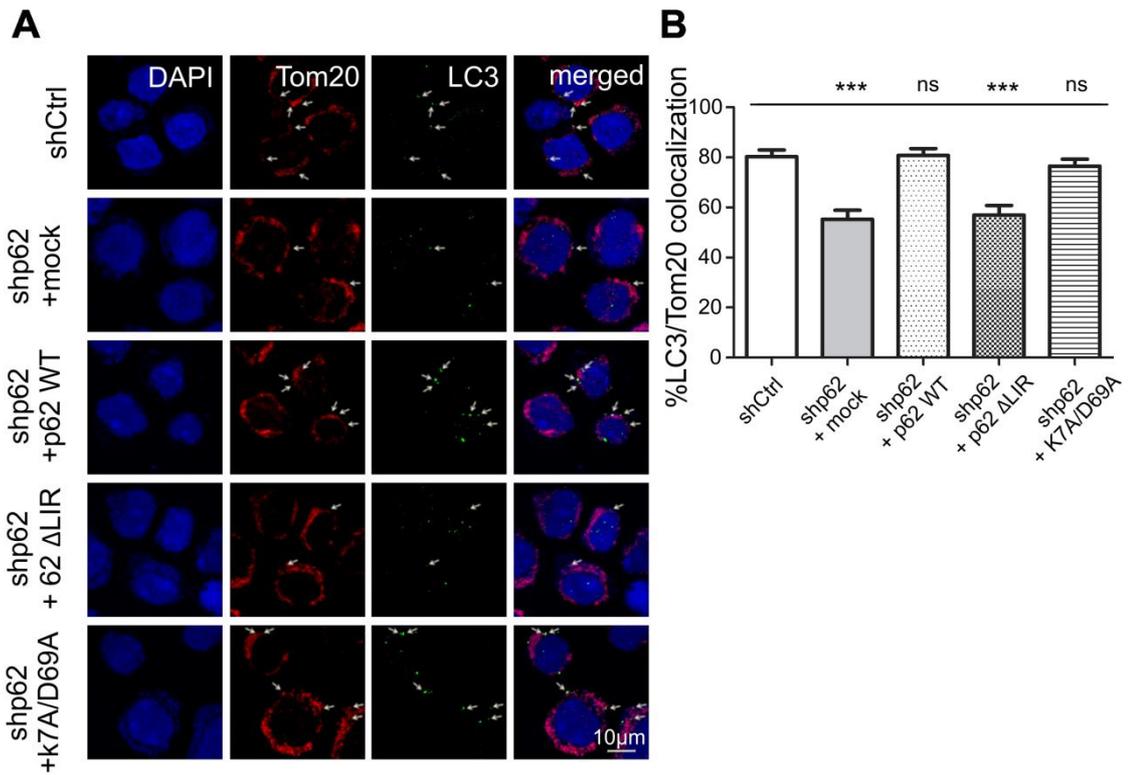
Figure 28. Mitophagy analysis of rescue experiment. (A) Co-localization of mitochondrial (Tom20) and autophagic (LC3) marker after treatment with DFP in shCtrl, shp62 and p62 mutants transduced MN1-driven leukemia cells was visualized by immunofluorescent staining. Arrows indicate co-localization of both markers. DAPI was used as a nuclear counterstain. Scale bar = 10 µm. (B) Co-localization of Tom20 and LC3 was analyzed by ImageJ (n = 50 for each group). Values are means ± SEM (ns: not significant; * $p \leq 0.05$; ** $p \leq 0.01$; *** $p \leq 0.001$).

These results strongly suggest that impaired proliferation in p62^{-/-} leukemia cells is mainly autophagy-dependent and involves mitophagy.

5. Discussion

This study identifies the selective autophagy receptor p62 as a key component required for rapid leukemia development. By using a murine AML model, it was demonstrated that loss of p62 reduced proliferation of leukemia cells and delayed leukemia development in mice, primarily caused by impaired mitochondrial function and altered energy homeostasis. In agreement with this, high p62 mRNA expression was associated with poor prognosis in human AML. Importantly, it was demonstrated that p62 is required for mitophagic clearance and maintenance of mitochondrial respiration. Thus, these results highlight the prominent role of selective autophagy in leukemia development and its importance of mitophagy to maintain mitochondrial integrity.

5.1 Selective autophagy in leukemia

Numerous recent studies have underlined the particular relevance of bulk autophagy in leukemia. It has been shown that autophagy protects murine HSCs from metabolic stress (Warr et al., 2013) to sustain HSC function (Ho et al., 2017) and to prevent leukemic transformation (Mortensen et al., 2011). Furthermore, a whole exome sequencing analysis on human AML samples revealed genetic aberrations in autophagy genes (including p62) in 14% of the cases studied (Visconte et al., 2017), suggesting that a defective autophagy machinery may be implicated in human leukemia development. On the contrary, it has been demonstrated that established leukemia requires autophagy for its maintenance, as knockdown of ATG3 (an essential autophagy protein) impaired BCR-ABL mediated chronic myeloid leukemia (Altman et al., 2011). Furthermore, Sumitomo and colleagues were able to prove that autophagy is essential for maintenance of acute myeloid leukemia-initiating cells (LICs), as loss of ATG5 or ATG7 prolonged survival in leukemic mice and reduced functional LICs (Sumitomo et al., 2016).

5. Discussion

Quality control is an important function of selective autophagy to protect normal and malignant cells from oxidative and genotoxic stress, including the efficient removal of dysfunctional mitochondria by mitophagy (Chourasia et al., 2015). Conditions that impair selective autophagy have been proposed to promote mutagenesis and cancer initiation (Dikic et al., 2010; White, 2012). However, the exact role of selective autophagy in cancer, especially in acute myeloid leukemia, remains elusive.

As presented in this study, loss of the selective autophagy receptor p62 compromises cellular homeostasis of leukemic cells under oncogenic stress and thereby delays leukemia development. Similar findings were observed in different cancer types. In oral carcinogenesis, p62 excess is more prominent in carcinomas than in normal tissues and may contribute to the resistance against cytotoxic stresses caused by radiation and chemotherapy. Knockdown of p62 in oral cancer cells inhibits cell growth, accumulates ROS under stress condition but does not induce apoptosis, which is consistent with our results shown in Figure 6,7,8,9 and 21. Another recent study has demonstrated that p62 loss in an mTORC1-driven renal cancer model reduced the kidney cystogenesis and cystadenoma formation (Lam et al., 2017). Similar observations were found in the *in vivo* transplantation experiments of this thesis, where loss of p62 attenuated leukemia development (Figure 14). In summary, these data suggest that p62 appears to be critical for oncogene-driven tumorigenesis including AML. Moreover, re-transplantation experiments of this study demonstrated that loss of p62 attenuated leukemia progression (Figure 16). This is in line with findings from a study in colorectal cancer which revealed that knockdown of p62 has inhibitory effects in a xenograft tumor model (Ren et al., 2014).

Another important finding of this thesis was the observation that high p62 expression correlated with shorter survival in adult patients with *de novo* AML (Figure 5). Interestingly, p62 was found to be highly expressed in certain cancer types (Inui et al., 2013; Iwadate et al., 2014; Iwadate et al., 2015; Ren et al., 2014) and was associated with poor prognosis in carcinoma of the ovary and endometrium as well as in head and neck cancer (Inui et al., 2013;

Iwadate et al., 2014; Iwadate et al., 2015). However, these studies were not able to address the question why p62 expression is increased in those tumor types. Yet, one study of non-small cell lung cancer indicated that high p62 expression reflects deregulated autophagy as expression of Beclin1 was found to be reduced (Wang et al., 2015). Allelic loss of the essential autophagy gene Beclin1 is commonly found in human cancer (Levine and Kroemer, 2008) suggesting that autophagy functions as a tumor-suppression mechanism. Therefore, it could be proposed that accumulation of p62 caused by deregulated autophagy might contribute to tumorigenesis (Mathew et al., 2009). In another cancer model, Umemura *et al.* showed that overexpression of p62 in liver is sufficient to induce hepatocellular carcinogenesis via Keap1-Nrf2 and mTOR signaling pathway (Umemura et al., 2016). Conversely, Inui *et al.* showed that p62 loss in oral cancer does not affect Keap1-Nrf2 pathway but rather reduces the content of antioxidant Glutathione leading to ROS accumulation and growth deficiency (Inui et al., 2013). This suggests that p62 protects the oral cancer cells from oxidative stress independently from Nrf2-Keap1 pathway. Notably, Glutathione is known to be located in different cellular compartment including the mitochondria, where it functions as a barrier against mitochondrial respiration-induced ROS (Ribas et al., 2014), suggesting the correlation between p62 loss and mitochondrial functionality in this cancer type.

5.2 The role of selective autophagy receptor p62 in mitochondrial function

Previous studies have claimed the important role of p62 in mitochondria, as absence of p62 causes fragmentation of mitochondria (Seibenhener et al., 2013) accompanied by fewer and shorter cristae (Muller et al., 2013). Similar morphological changes of mitochondria in MN1-driven leukemia cells (Figure 19 and 20) were also observed in this thesis. Furthermore, mitochondrial fragmentation is associated with loss of membrane potential (Chen et al., 2005), impaired mitochondrial energetics (Guillery et al., 2008) and damage

5. Discussion

of mitochondrial DNA (Gilkerson et al., 2000), anticipating mitochondrial dysfunction (Seibenhener et al., 2013). In brown adipose tissue, p62 has been shown as a regulator of mitochondrial integrity and functionality. Accordingly, mitochondrial functions of p62$^{-/-}$ adipocytes are impaired, shown by decreased oxidative capacity and aberrant genetic program responsible for mitochondrial biogenesis (Muller et al., 2013). In renal cancer, increased mitochondrial ROS and reduced mitochondrial maximal respiration were found in p62$^{-/-}$ tumor cells, indicating that p62 loss provoked accumulation of damaged mitochondria (Lam et al., 2017). In line with this, reduced mitochondrial mass (Figure 24A), increased mitochondrial ROS levels (Figure 21A) and reduced mitochondrial respiration capacity (Figure 22) were observed in this thesis, evidences for mitochondrial dysfunction in p62$^{-/-}$ MN1-driven ldMBM leukemia cells.

Although cancer cells frequently generate higher ROS levels than healthy cells (Sullivan and Chandel, 2014), the amount of mitochondrial ROS in MN1-induced leukemia cells and their comparable HSC compartment in normal hematopoiesis were almost equal (Figure 21A). Moreover, normal HSCs of p62$^{-/-}$ mice tended to even lower mitochondrial ROS levels than WT mice. This suggests that only under oncogenic stress conditions HSCs depend on p62 to maintain mitochondrial homeostasis.

However, the underlying mechanism of how p62 protects the leukemia cells against mitochondrial ROS remains unknown. As mentioned, p62 is involved in the Keap1-Nrf2 pathway which regulates antioxidative stress response. This includes also ROS production by mitochondria (Kovac et al., 2015). Under cytotoxic stress conditions, p62 leads to binding and degradation of Keap1, which subsequently stabilizes Nrf2 followed by an antioxidative stress response (Ichimura et al., 2013). Hence, loss of p62 may increase mitochondrial ROS by impairment of Nrf2 activation, however this requires further investigations. Besides antioxidative stress signaling pathways, increased ROS levels can also be explained by accumulation of dysfunctional mitochondria caused by impaired degradation. Of note, the major degradation pathway in mitochondrial turnover is mitophagy (Kim et

al., 2007), which utilizes p62 as a selective autophagy receptor (Geisler et al., 2010).

5.3 The role of selective autophagy receptor p62 in mitophagy

Growing lines of evidence demonstrate that mitophagy may be the missing link between mitochondrial dysfunction and p62 deficiency. As an example, knockdown of p62 in renal cancer leads to increased expression of mitochondrial protein kinase PINK1, a marker for mitophagy (Lam et al., 2017).

Selective degradation of mitochondria by autophagy, known as mitophagy, is a cellular quality control mechanism necessary to remove dysfunctional mitochondria (Youle and Narendra, 2011). Mounting evidences link p62 to clustering of damaged mitochondria (Narendra et al., 2010a; Okatsu et al., 2010). Previous studies have implicated p62 in selective turnover of mitochondria by mitophagy (Geisler et al., 2010; Heo et al., 2015; Lazarou et al., 2015; Matsumoto et al., 2015; Richter et al., 2016). Interactome analysis of this study revealed that inhibition of the autophagic degradation pathway caused enrichment of all detected mitochondrial candidates (Figure 18B). TMEM160, one of the mitochondrial proteins with the highest accumulation after autophagy inhibition, was already previously described as a potential interaction partner of p62 in a proteomic analysis of the autophagy interaction network (Behrends et al., 2010). Three additional detected mitochondrial proteins had comparable high values as Keap1, which is known to facilitate p62-mediated aggregate clearance via autophagy (Fan et al., 2010) and emphasizes the aspect of autophagy-dependent binding of p62 to mitochondria. Moreover, the results from this thesis revealed that mitochondrial damage induced by iron loss caused by DFP triggered degradation of COXIV accompanied with upregulation of p62 and LC3II in MN1-driven leukemia cells. Finally, loss of p62 caused reduced translocation

of mitochondria to autophagosomes (Figure 26), resulting in an accumulation of damaged mitochondria (Figure 21 and 22).

More recently, it has been questioned as to what extent p62 is actually involved in mitophagy (Narendra et al., 2010; Lazarou et al., 2015; Heo et al., 2015). It has been shown that mitophagy can involve the mitochondrial protein kinase PINK1 and the cytoplasmic ubiquitin ligase Parkin, which are mutated in certain forms of Parkinson's disease (Narendra et al., 2010a). These studies suggest that the autophagy receptors Optineurin and NDP52, but not p62, are required for PINK1/Parkin-mediated mitophagy (Heo et al., 2015; Lazarou et al., 2015). However, these studies focus solely on a particular type of mitophagy depending on Parkin overexpression, as it has been shown that endogenous Parkin is not sufficient to induce mitophagy (Rakovic et al., 2013). In contrast, p62 demonstrated here its important role in PINK1/Parkin-independent mitophagy of MN1-driven leukemia. Rescue experiments with a p62 mutant lacking the LIR domain and therefore disrupting its binding to autophagosomes displayed significantly reduced translocation of mitochondria to autophagosomes after DFP treatment (Figure 28) in a PINK1/Parkin-independent fashion (Allen et al., 2013). However, further studies are needed to clarify which autophagy receptor is preferentially used in PINK1/Parkin-dependent mitophagy in leukemia.

5.4 Mitochondrial dependency in AML development and maintenance

Mitochondria generate ATP by oxidative phosphorylation, which is required for cell proliferation and tumorigenesis. Indeed, growing evidences showed that AML pathogenesis strongly relies on mitochondrial function (Basak and Banerjee, 2015). Previous reports exhibit that AML displays higher mitochondrial biogenesis and respiration capacity compared to normal hematopoietic stem cells (Skrtic et al., 2011). Interestingly, by targeting mitochondrial translation with the antibiotic tigecycline, the authors were able to prove that primary AML cells were more effectively killed than normal

hematopoietic stem cells (Skrtic et al., 2011). Consistent with these data, Lee et al. demonstrated that treatment with the compound avocadin B caused mitochondrial dysfunction leading to ROS-dependent leukemia cell death, without effecting normal hematopoiesis (Lee et al., 2015). These findings underlie the mitochondrial dependency in AML maintenance.

Turnover of dysfunctional mitochondria is tightly regulated by mitophagy to maintain mitochondrial function and integrity. Recently, it was demonstrated that inactivation of autophagy through knockdown of ATG7 alters viability of BCR-ABL-positive leukemia cells due to altered mitochondrial energy metabolism accompanied by accumulation of mitochondrial ROS caused by impaired autophagy-mediated degradation of mitochondria (Karvela et al., 2016). Although this paper describes the process of non-selective autophagy, similar findings were observed in this thesis showing that increased ROS and accumulation of dysfunctional mitochondria correlated with prolonged survival in p62$^{-/-}$ leukemic mice (Figure 21B). Importantly, reduced proliferation capacity of p62$^{-/-}$ MN1-driven leukemia cells was found to be autophagy-dependent (Figure 27 and 28).

Taken together, mitochondrial homeostasis is tightly controlled by p62-dependent mitophagy in AML development and maintenance.

5.5 Outlook

Although the role of p62 as a mitophagy receptor in the context of leukemia has been intensively investigated in this thesis, there are still unanswered questions. One open question addresses the relation between hypoxia and autophagy under loss of p62, as leukemia cells normally proliferate in the bone marrow, where oxygen supply is limited (Tabe and Konopleva, 2014). Low oxygen concentration has been shown to induce mitophagy in solid tumors protecting them from increased ROS production under hypoxia and support cellular fitness (Zhang and Ney, 2009). Whether hypoxia in the bone marrow may also contribute to leukemia progression under loss of mitophagy will require further investigation and could provide a better understanding of

how selective autophagy protects leukemia cells from hypoxia-induced stress.

Another more important question addresses the possibility of p62 participating in additional selective autophagy types beside mitophagy. This is supported by the fact that the SILAC interactome analysis from this thesis revealed other putative non-mitochondrial interaction partners of p62 derived from the aggresome and the ER. Of note, it has been shown that p62 is involved in degradation of polyubiquitinated protein aggregate (Bjorkoy et al., 2005; Gamerdinger et al., 2009; Pankiv et al., 2007). Further studies are needed to clarify its role in AML. Autophagic degradation of the ER is still not broadly analyzed, but a novel selective autophagy receptor FAM134b for ER-phagy has been recently identified (Khaminets et al., 2015). From the current literature, there is no information about p62 in the context of ER-phagy, despite the findings from this thesis based on the interactome analysis. Therefore, further investigations are required to clarify if p62 also contributes in ER-phagy.

5.6 Conclusions

In conclusion, this study demonstrates for the first time the fundamental role of selective autophagy as a quality control mechanism in leukemia development (summarized in Figure 29). In the context of oncogene-induced stress, p62 is required to bring damaged mitochondria to the autophagosome, followed by mitophagy and rapid leukemia development. Loss of p62 failed to protect HSCs from oncogenic stress causing ineffective elimination of damaged mitochondria and mitochondrial superoxide accumulation. Subsequently, this impairs survival of leukemia cells and delays leukemia development. These findings provide a mechanism-based rationale for the development of drugs targeting selective autophagy in leukemia.
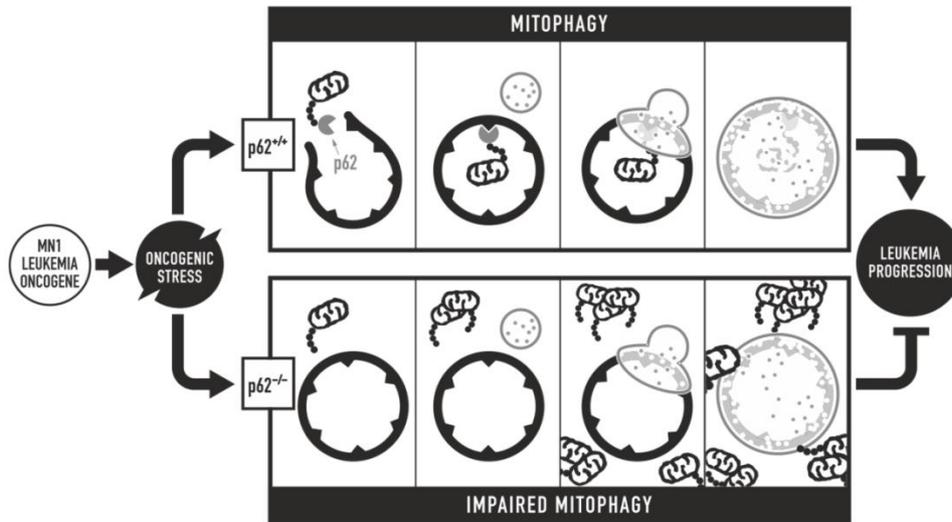
Figure 29. Model of p62-mediated mitophagy in acute myeloid leukemia development. Under oncogenic stress, p62 is required for (i) efficient removal of damaged mitochondria by mitophagy and (ii) rapid leukemia progression (upper panel). In the absence of p62, damaged mitochondria accumulate, leading to impaired mitochondrial function and reduced leukemia progression (lower panel).

6. Summary

Acute myeloid leukemia (AML) is a clonal malignancy of hematopoietic stem cells (HSCs) characterized by expansion of myeloid blasts in the bone marrow. It has been shown that autophagy is a degradative process, which delivers cytoplasmic components to lysosomes to prevent malignant transformation by maintaining HSC integrity. Besides its function as a bulk degradation machinery to recycle cytoplasmic components during limited energy supply, autophagy also serves as an intracellular quality control mechanism. Selective autophagy requires autophagy receptors such as p62 to specifically bridge the targeted cargos into autophagosomes. p62 is known as a central signaling hub involved in pro-oncogenic signaling pathways and autophagic degradation pathways. However, little is known about the role of p62 as a selective autophagy receptor in AML. This study aims to elucidate the precise function of p62 as an autophagy receptor in leukemia development and maintenance.

In silico analysis revealed that high p62 expression was significantly associated with poor overall survival of adult patients with *de novo* AML, suggesting that p62 may promote leukemia maintenance. To address the functional role of p62 in leukemia, genome editing by CRISPR/Cas9 was used to knockout p62 in four human AML cell lines. Importantly, p62 loss reduced cell proliferation in all four cell lines. This observation could be transferred to a murine leukemia cell model in which leukemic transformation of lineage-depleted bone marrow (ldMBM) cells was induced by overexpression of the human transcriptional coactivator MN1. Knockdown of p62 by shRNA in MN1-driven leukemia cells impaired proliferation and decreased colony forming ability without altering apoptosis. This indicates that p62 is crucial for leukemia proliferation *in vitro*. To further characterize the role of p62 in leukemia development and maintenance a murine AML transplantation model was established. Therefore, ldMBM cells isolated from WT and p62$^{-/-}$ mice were transduced with MN1 and transplanted into lethally irradiated mice. As expected, all mice developed fatal myeloid proliferation. Notably, p62 loss in MN1-driven leukemia significantly prolonged survival in

6. Summary

mice and caused a more immature phenotype. Consistent with the *in vitro* results, *ex vivo* analysis of p62$^{-/-}$ leukemic cells displayed decreased colony-forming ability, although p62 loss did not affect composition and function of HSCs. Moreover, re-transplantation of primary MN1-driven leukemia cells attenuated leukemia progression upon p62 loss. These findings support a decisive role of p62 in leukemia development and maintenance.

To gain molecular insight into the function of p62 during myeloid transformation an interactome analysis of murine MN1-driven leukemia cells was performed. This revealed first that p62 predominantly interacts with mitochondrial proteins and second that inhibition of autophagic degradation causes accumulation of p62-bound mitochondria. This leads to the first assumption that loss of p62 may provoke mitochondrial accumulation with increasing mitochondrial damage and second that p62 may mediate degradation of mitochondria by mitophagy. Indeed, in the absence of p62, accumulation of dysfunctional mitochondria was detected by morphological changes of the mitochondria, increased mitochondrial ROS and impaired mitochondrial respiration capacity. Furthermore, induction of PINK1/Parkin-independent mitophagy revealed that loss of p62 caused impaired degradation of mitochondrial proteins and reduced translocation of damaged mitochondria into autophagosomes. Taken together, p62 is required for effective degradation of dysfunctional mitochondria by mitophagy in AML.

Due to the fact that p62 is a multifunctional protein, rescue experiments with different mutants of p62 were performed to clarify if p62-mediated mitophagy contributes to leukemia proliferation. Notably, the autophagy-deficient mutant (disabled to bind autophagosomes) reduced cell growth and colony-forming ability to the same extent as knockdown of p62, as the clustering-deficient mutant (disabled to form aggregates) displayed an intermediate phenotype. Strikingly, only the autophagy-deficient mutant failed to rescue mitophagy.

In conclusion, this study demonstrates the prominent role of p62 as a selective autophagy receptor for mitochondrial quality control which contributes to leukemia development and maintenance. Therefore, targeting selective autophagy opens new venues in the treatment of AML.

7. Zusammenfassung

Die akute myeloische Leukämie (AML) ist eine maligne Erkrankung myeloischer Vorläuferzellen des Knochenmarkes. Durch die klonale Expansion primitiver myeloischer Blasten im Knochenmark kommt es zur Verdrängung der normalen Blutbildung mit Verdrängung der normalen Hämatopoese. Die AML zählt zu den häufigsten akuten Leukämien im Erwachsenalter, deren Krankheitsverlauf akut auftritt, rasch progredient ist und unbehandelt tödlich endet. Die AML entsteht durch maligne Transformation myeloischer Vorläuferzellen als Folge genetischer Mutationen und epigenetischer Veränderungen. Hierdurch kommt es zur gesteigerten Proliferation, Schutz vor Apoptose und gehemmter Differenzierung. Jüngste Studien konnten zeigen, dass der Degradationsprozess der Autophagie bei der Leukämieentwicklung eine wichtige Rolle spielt.

Autophagie ist ein evolutionär konservierter Prozess, der den Abbau zellulärer Proteinkomplexe und Organellen zur Energiegewinnung bewirkt. Dieser Recyclingprozess sichert somit das Überleben der Zellen, wenn diese zellulären Stressbedingungen wie Nährstoffentzug ausgesetzt sind. Darüber hinaus fungiert Autophagie auch als ein zelluläres Qualitätskontrollsystem, das die gezielte Beseitigung toxischer Zellbestandteile, wie Proteinaggregate und beschädigter oder überflüssiger Organellen reguliert. Die selektive Form der Autophagie stellt dabei einen besonderen molekularen Mechanismus dar, der die Beteiligung von spezifischen Rezeptoren voraussetzt, die Adaptorfunktionen aufweisen. p62/SQSTM1 (sequestosome 1, nachfolgend p62 genannt) ist einer der am besten charakterisierten Autophagierezeptoren: p62 ist an der selektiven Autophagie von Proteinaggregaten (Aggrephagie), Peroxisomen (Pexophagie) und Mitochondrien (Mitophagie) beteiligt. Von besonderer Bedeutung ist außerdem die Interaktion von p62 mit NFκB-, mTOR- und Keap1/Nrf2-Signalwegen. So konnte gezeigt werden, dass p62 einen NFκB-abhängigen Überlebensvorteil bei der Promyelozytenleukämie unter ATRA (all-trans-Retinsäure)-Behandlung hervorruft. Im Rahmen dieser Dissertation haben

wir untersucht, welche Rolle die selektive Autophagie - und im speziellen p62 - bei der Leukämieentstehung spielt.

Eine *in silico* Analyse unter Einbeziehung von mRNA-Expressions- und Überlebensdaten von 173 Patienten mit *de novo* AML aus der TCGA-Datenbank ergab, dass hohe Expressionswerte für p62 mit einem signifikant schlechterem Gesamtüberleben assoziiert waren.

Um den Einfluss von p62 auf das Zellwachstum im Kontext der AML funktionell zu untersuchen, wurde ein CRISPR/Cas9-vermittelter Knockout von p62 in vier verschiedenen humanen AML Zelllinien durchgeführt. Der Verlust von p62 führte zu einer signifikanten Abnahme der Proliferation in allen getesteten Zelllinien. Zur weiteren Charakterisierung von p62 erfolgte zunächst die Generierung einer murinen Leukämiezelllinie durch Expression des humanen Transkriptionsfaktors MN1. Auch hier zeigte der Knockdown von p62 eine Inhibierung des Zellwachstums. Funktionelle Analysen ergaben außerdem, dass der p62-Verlust zur Reduktion der Kolonienbildung führte, ohne dass dabei ein vermehrter Zelltod oder eine gehemmte Zellsynthese beobachtet werden konnten.

Um einen direkten Zusammenhang zwischen p62 und der Leukämieentwicklung zu untersuchen, wurde ein AML-Mausmodel etabliert. Hierfür wurden *lineage*-negative Knochenmarkzellen von Wildtyp- und p62$^{-/-}$ - Mäusen mit dem Onkogen MN1 transduziert und in letal bestrahlte Wildtyp-Empfängermäuse transplantiert. Alle Mäuse entwickelten eine AML, wobei es signifikante Unterschiede im zeitlichen Auftreten der Leukämie gab: leukämiekranke p62$^{-/-}$-Mäuse zeigten ein deutlich längeres Gesamtüberleben als Mäuse der entsprechenden Kontrollgruppe. Detaillierte *post mortem*-Analysen ergaben, dass leukämiekranke p62$^{-/-}$-Mäuse höhere weiße Blutzellen sowie erniedrigte roten Blutzellen im peripheren Blut aufwiesen und dabei vermehrt undifferenzierte Blasten im Knochenmark aufwiesen. Dies spiegelte sich in den durchflußzytometrischen Analysen durch eine Zunahme der *lineage*$^{-}$- (Lin^{-}) und Lin^{-}cKit^{+}-Populationen sowie eine Verminderung der CD11b^{+}-Population wieder. Funktionelle Analysen ergaben, dass die Koloniebildung der p62$^{-/-}$-Leukämiezellen erkrankter

7. Zusammenfassung

Mäuse deutlich reduziert war, obwohl der alleinige Verlust von p62 keinen Einfluss auf die Zusammensetzung und Funktion normaler hämatopoetischer Stammzellen (HSCs) hatte. Die sekundäre Re-Transplantation von MN1-exprimierenden Leukämiezellen (aus den primären Transplantationen) zeigte erneut eine deutlich längere Latenz der p62$^{-/-}$-Leukämien. Diese Beobachtung bestätigt, dass der Verlust von p62 auch eine Rolle im Erhalt des leukämischen Phänotyps hat.

Um den zugrundeliegenden molekularen Mechanismus der p62-abhängigen leukämischen Transformation aufzudecken, erfolgte eine proteomische Analyse der p62-Interaktionspartner in MN1-exprimierenden Leukämiezellen mittels SILAC (*stable isotope labeling by amino acids in cell culture*). Diese führte zur Identifizierung von 31 p62-Interaktionspartnern, welche neben bekannten (p62 selbst, Keap1) auch unbekannte p62-Interaktionspartner umfasste. Die häufigsten Interaktionspartner waren mit 35% membran- als auch matrixgebundene mitochondriale Proteine. Die übrigen p62-Interaktoren waren im endoplasmatischen Retikulum, in Aggresomen, und im Zytoplasma lokalisiert sowie Bestandteile zellulärer Membranen und Exosomen. Darüber hinaus zeigte sich eine starke Autophagieabhängigkeit in der Interaktion zwischen p62 und Mitochondrien, da eine pharmakologische Hemmung der Autophagie mit Bafilomycin A1 zur Anreicherung aller detektierten mitochondrialen Proteine führte. Diese Ergebnisse ließen vermuten, dass p62 für die Elimination defekter Mitochondrien notwendig ist.

In der Tat fanden sich zahlreiche Hinweise für mitochondriale Dysfunktion in Abwesenheit von p62. Eine Methode zur Überprüfung der Mitochondrienfunktion erfolgte über Messung von mitochondrialem ROS (*reactive oxygen species*). Interessanterweise, hatte die Abwesenheit von p62 keinen Einfluss auf den ROS-Gehalt gesunder HSCs, jedoch kam es zu einer signifikanten Anreicherung von ROS in den p62$^{-/-}$-Blasten leukämiekranker Mäuse verglichen zur Kontrollgruppe. Zur weiteren Validierung dieser Ergebnisse erfolgte die Sauerstoffverbrauchsmessung, auch OCR (*oxygen consumption rate)* genannt, zur Bestimmung der

Mitochondrienfunktion. Hier bestätigte sich, dass Mitochondrien in p62$^{-/-}$-Blasten leukämiekranker Mäuse eine deutlich reduzierte Sauerstoffkapazität aufwiesen, was für mitochondriale Dysfunktion spricht. Diese Daten unterstreichen somit die bedeutende Rolle von p62 in der Aufrechterhaltung der mitochondrialen Homöostase.

Zur Untersuchung der mitochondrialen Degradation mittels Mitophagie wurden MN1-exprimierende Leukämiezellen mit dem Eisenchelator Deferiprone (DFP) behandelt, der nachweislich eine Schädigung der Mitochondrien auslöst und eine PINK1/Parkin-unabhängige Mitophagie induziert. Die DFP-Behandlung bewirkte in den Kontrollzellen den gewünschten mitochondrialen Abbau, während in den p62-Knockdown Zellen nur ein minimaler Mitochondrienabbau erfolgte. Zur visuellen Darstellung des Mitophagieprozesses wurden die geschädigten Mitochondrien in den Autophagosomen quantifiziert. Mittels Konfokalmikroskopie wurde die Kolokalisation des mitochondrialen Markers Tom20 mit dem autophagosomalen Marker LC3 bestimmt. Nach DFP-Behandlung lag die Kolokalisationsrate zwischen LC3 und Tom20 in den Kontrollzellen bei 72% und in den p62-Knockdown Zellen hingegen nur bei 54%. Hieraus lässt sich ableiten, dass Leukämiezellen für den effektiven Abbau geschädigter Mitochondrien durch Mitophagie auf p62 angewiesen sind.

Da p62 ein multifunktionales Protein mit unterschiedlichen Proteindomänen ist, wurde anhand von genetischen *Rescue*-Experimenten mit verschiedenen p62-Mutanten geklärt werden, ob spezifisch die p62-vermittelte Mitophagie Einfluss auf die Proliferation der Leukämiezellen hat. Es zeigte sich, dass die autophagie-defiziente p62-Mutante den Phänotyp des p62-Knockdowns nicht revertieren konnten (gemessen im Zellwachstum und der Koloniebildung), während Wildtyp-p62 hierzu in der Lage war. Des Weiteren zeigten die Kolokalisationsanalysen (mittels Konfokalmikroskopie), dass diese Effekte mitophagieabhängig waren, da es nur der autophagie-defizienten Mutante von p62 nicht gelang eine effektive Translokation der Mitochondrien in Autophagosomen zu vermitteln.

7. Zusammenfassung

Zusammengefasst konnte in dieser Arbeit gezeigt werden, dass p62 als selektiver Autophagierezeptor eine Schlüsselfunktion in der Aufrechterhaltung der mitochondrialen Homöostase einnimmt und dabei entscheidend zur Entstehung der Leukämie beiträgt.

8. References

Al Rawi, S., S. Louvet-Vallee, A. Djeddi, M. Sachse, E. Culetto, C. Hajjar, L. Boyd, R. Legouis, and V. Galy. 2011. Postfertilization autophagy of sperm organelles prevents paternal mitochondrial DNA transmission. *Science* 334:1144-1147.

Allen, G.F., R. Toth, J. James, and I.G. Ganley. 2013. Loss of iron triggers PINK1/Parkin-independent mitophagy. *EMBO reports* 14:1127-1135.

Altman, B.J., S.R. Jacobs, E.F. Mason, R.D. Michalek, A.N. MacIntyre, J.L. Coloff, O. Ilkayeva, W. Jia, Y.W. He, and J.C. Rathmell. 2011. Autophagy is essential to suppress cell stress and to allow BCR-Abl-mediated leukemogenesis. *Oncogene* 30:1855-1867.

Arber, D.A., A. Orazi, R. Hasserjian, J. Thiele, M.J. Borowitz, M.M. Le Beau, C.D. Bloomfield, M. Cazzola, and J.W. Vardiman. 2016. The 2016 revision to the World Health Organization classification of myeloid neoplasms and acute leukemia. *Blood* 127:2391-2405.

Ashford, T.P., and K.R. Porter. 1962. Cytoplasmic components in hepatic cell lysosomes. *The Journal of cell biology* 12:198-202.

Auberger, P., and A. Puissant. 2016. Autophagy, a key mechanism of oncogenesis and resistance in leukemia. *Blood*

Auten, R.L., and J.M. Davis. 2009. Oxygen toxicity and reactive oxygen species: the devil is in the details. *Pediatric research* 66:121-127.

Basak, N.P., and S. Banerjee. 2015. Mitochondrial dependency in progression of acute myeloid leukemia. *Mitochondrion* 21:41-48.

Behrends, C., and S. Fulda. 2012. Receptor proteins in selective autophagy. *International journal of cell biology* 2012:673290.

Behrends, C., M.E. Sowa, S.P. Gygi, and J.W. Harper. 2010. Network organization of the human autophagy system. *Nature* 466:68-76.

Birgisdottir, A.B., T. Lamark, and T. Johansen. 2013. The LIR motif - crucial for selective autophagy. *Journal of cell science* 126:3237-3247.

8. References

Bjorkoy, G., T. Lamark, A. Brech, H. Outzen, M. Perander, A. Overvatn, H. Stenmark, and T. Johansen. 2005. p62/SQSTM1 forms protein aggregates degraded by autophagy and has a protective effect on huntingtin-induced cell death. *The Journal of cell biology* 171:603-614.

Brand, M.D., and D.G. Nicholls. 2011. Assessing mitochondrial dysfunction in cells. *The Biochemical journal* 435:297-312.

Cassileth, P.A., D.P. Harrington, J.D. Hines, M.M. Oken, J.J. Mazza, P. McGlave, J.M. Bennett, and M.J. O'Connell. 1988. Maintenance chemotherapy prolongs remission duration in adult acute nonlymphocytic leukemia. *Journal of clinical oncology : official journal of the American Society of Clinical Oncology* 6:583-587.

Chen, H., A. Chomyn, and D.C. Chan. 2005. Disruption of fusion results in mitochondrial heterogeneity and dysfunction. *The Journal of biological chemistry* 280:26185-26192.

Chourasia, A.H., M.L. Boland, and K.F. Macleod. 2015. Mitophagy and cancer. *Cancer & metabolism* 3:4.

Colaprico, A., T.C. Silva, C. Olsen, L. Garofano, C. Cava, D. Garolini, T.S. Sabedot, T.M. Malta, S.M. Pagnotta, I. Castiglioni, M. Ceccarelli, G. Bontempi, and H. Noushmehr. 2016. TCGAbiolinks: an R/Bioconductor package for integrative analysis of TCGA data. *Nucleic acids research* 44:e71.

Coulombel, L. 2004. Identification of hematopoietic stem/progenitor cells: strength and drawbacks of functional assays. *Oncogene* 23:7210-7222.

Dicke, K.A., S.E. Tindle, F.M. Davis, S. Jagannath, S. Tucker, M. Lilien, P. van Leeuwen, D.S. Verma, and L. Vellekoop. 1983. Leukemic cell colony formation in soft agar by bone marrow cells and peripheral blood cells from untreated acute leukemia patients. *Experimental hematology* 11:341-350.

Dikic, I., T. Johansen, and V. Kirkin. 2010. Selective autophagy in cancer development and therapy. *Cancer research* 70:3431-3434.

8. References

Dohner, H., E.H. Estey, S. Amadori, F.R. Appelbaum, T. Buchner, A.K. Burnett, H. Dombret, P. Fenaux, D. Grimwade, R.A. Larson, F. Lo-Coco, T. Naoe, D. Niederwieser, G.J. Ossenkoppele, M.A. Sanz, J. Sierra, M.S. Tallman, B. Lowenberg, and C.D. Bloomfield. 2010. Diagnosis and management of acute myeloid leukemia in adults: recommendations from an international expert panel, on behalf of the European LeukemiaNet. *Blood* 115:453-474.

Dohner, H., D.J. Weisdorf, and C.D. Bloomfield. 2015. Acute Myeloid Leukemia. *The New England journal of medicine* 373:1136-1152.

Dupont, N., S. Lacas-Gervais, J. Bertout, I. Paz, B. Freche, G.T. Van Nhieu, F.G. van der Goot, P.J. Sansonetti, and F. Lafont. 2009. Shigella phagocytic vacuolar membrane remnants participate in the cellular response to pathogen invasion and are regulated by autophagy. *Cell host & microbe* 6:137-149.

Duran, A., R. Amanchy, J.F. Linares, J. Joshi, S. Abu-Baker, A. Porollo, M. Hansen, J. Moscat, and M.T. Diaz-Meco. 2011. p62 is a key regulator of nutrient sensing in the mTORC1 pathway. *Molecular cell* 44:134-146.

Duran, A., J.F. Linares, A.S. Galvez, K. Wikenheiser, J.M. Flores, M.T. Diaz-Meco, and J. Moscat. 2008. The signaling adaptor p62 is an important NF-kappaB mediator in tumorigenesis. *Cancer cell* 13:343-354.

Elmore, S.P., T. Qian, S.F. Grissom, and J.J. Lemasters. 2001. The mitochondrial permeability transition initiates autophagy in rat hepatocytes. *FASEB journal : official publication of the Federation of American Societies for Experimental Biology* 15:2286-2287.

Fan, W., Z. Tang, D. Chen, D. Moughon, X. Ding, S. Chen, M. Zhu, and Q. Zhong. 2010. Keap1 facilitates p62-mediated ubiquitin aggregate clearance via autophagy. *Autophagy* 6:614-621.

Farre, J.C., and S. Subramani. 2016. Mechanistic insights into selective autophagy pathways: lessons from yeast. *Nature reviews. Molecular cell biology* 17:537-552.

8. References

Funderburk, S.F., Q.J. Wang, and Z. Yue. 2010. The Beclin 1-VPS34 complex--at the crossroads of autophagy and beyond. *Trends in cell biology* 20:355-362.

Galluzzi, L., F. Pietrocola, J.M. Bravo-San Pedro, R.K. Amaravadi, E.H. Baehrecke, F. Cecconi, P. Codogno, J. Debnath, D.A. Gewirtz, V. Karantza, A. Kimmelman, S. Kumar, B. Levine, M.C. Maiuri, S.J. Martin, J. Penninger, M. Piacentini, D.C. Rubinsztein, H.U. Simon, A. Simonsen, A.M. Thorburn, G. Velasco, K.M. Ryan, and G. Kroemer. 2015. Autophagy in malignant transformation and cancer progression. *The EMBO journal* 34:856-880.

Gamerdinger, M., P. Hajieva, A.M. Kaya, U. Wolfrum, F.U. Hartl, and C. Behl. 2009. Protein quality control during aging involves recruitment of the macroautophagy pathway by BAG3. *The EMBO journal* 28:889-901.

Geisler, S., K.M. Holmstrom, D. Skujat, F.C. Fiesel, O.C. Rothfuss, P.J. Kahle, and W. Springer. 2010. PINK1/Parkin-mediated mitophagy is dependent on VDAC1 and p62/SQSTM1. *Nature cell biology* 12:119-131.

Gilkerson, R.W., D.H. Margineantu, R.A. Capaldi, and J.M. Selker. 2000. Mitochondrial DNA depletion causes morphological changes in the mitochondrial reticulum of cultured human cells. *FEBS letters* 474:1-4.

Guillery, O., F. Malka, P. Frachon, D. Milea, M. Rojo, and A. Lombes. 2008. Modulation of mitochondrial morphology by bioenergetics defects in primary human fibroblasts. *Neuromuscular disorders : NMD* 18:319-330.

Heo, J.M., A. Ordureau, J.A. Paulo, J. Rinehart, and J.W. Harper. 2015. The PINK1-PARKIN Mitochondrial Ubiquitylation Pathway Drives a Program of OPTN/NDP52 Recruitment and TBK1 Activation to Promote Mitophagy. *Molecular cell* 60:7-20.

Heuser, M., B. Argiropoulos, F. Kuchenbauer, E. Yung, J. Piper, S. Fung, R.F. Schlenk, K. Dohner, T. Hinrichsen, C. Rudolph, A. Schambach, C. Baum, B. Schlegelberger, H. Dohner, A. Ganser, and R.K. Humphries. 2007. MN1 overexpression induces acute myeloid leukemia in mice and predicts ATRA resistance in patients with AML. *Blood* 110:1639-1647.

8. References

Ho, T.T., M.R. Warr, E.R. Adelman, O.M. Lansinger, J. Flach, E.V. Verovskaya, M.E. Figueroa, and E. Passegue. 2017. Autophagy maintains the metabolism and function of young and old stem cells. *Nature* 543:205-210.

Huo, Y., H. Cai, I. Teplova, C. Bowman-Colin, G. Chen, S. Price, N. Barnard, S. Ganesan, V. Karantza, E. White, and B. Xia. 2013. Autophagy opposes p53-mediated tumor barrier to facilitate tumorigenesis in a model of PALB2-associated hereditary breast cancer. *Cancer discovery* 3:894-907.

Ichimura, Y., T. Kumanomidou, Y.S. Sou, T. Mizushima, J. Ezaki, T. Ueno, E. Kominami, T. Yamane, K. Tanaka, and M. Komatsu. 2008. Structural basis for sorting mechanism of p62 in selective autophagy. *The Journal of biological chemistry* 283:22847-22857.

Ichimura, Y., S. Waguri, Y.S. Sou, S. Kageyama, J. Hasegawa, R. Ishimura, T. Saito, Y. Yang, T. Kouno, T. Fukutomi, T. Hoshii, A. Hirao, K. Takagi, T. Mizushima, H. Motohashi, M.S. Lee, T. Yoshimori, K. Tanaka, M. Yamamoto, and M. Komatsu. 2013. Phosphorylation of p62 activates the Keap1-Nrf2 pathway during selective autophagy. *Molecular cell* 51:618-631.

Inui, T., T. Chano, M. Takikita-Suzuki, M. Nishikawa, G. Yamamoto, and H. Okabe. 2013. Association of p62/SQSTM1 excess and oral carcinogenesis. *PloS one* 8:e74398.

Itakura, E., and N. Mizushima. 2011. p62 Targeting to the autophagosome formation site requires self-oligomerization but not LC3 binding. *The Journal of cell biology* 192:17-27.

Iwadate, R., J. Inoue, H. Tsuda, M. Takano, K. Furuya, A. Hirasawa, D. Aoki, and J. Inazawa. 2014. High Expression of SQSTM1/p62 Protein Is Associated with Poor Prognosis in Epithelial Ovarian Cancer. *Acta histochemica et cytochemica* 47:295-301.

Iwadate, R., J. Inoue, H. Tsuda, M. Takano, K. Furuya, A. Hirasawa, D. Aoki, and J. Inazawa. 2015. High Expression of p62 Protein Is Associated with Poor Prognosis and Aggressive Phenotypes in Endometrial Cancer. *The American journal of pathology* 185:2523-2533.

8. References

Jain, A., T. Lamark, E. Sjottem, K.B. Larsen, J.A. Awuh, A. Overvatn, M. McMahon, J.D. Hayes, and T. Johansen. 2010. p62/SQSTM1 is a target gene for transcription factor NRF2 and creates a positive feedback loop by inducing antioxidant response element-driven gene transcription. *The Journal of biological chemistry* 285:22576-22591.

Johansen, T., and T. Lamark. 2011. Selective autophagy mediated by autophagic adapter proteins. *Autophagy* 7:279-296.

Joung, I., J.L. Strominger, and J. Shin. 1996. Molecular cloning of a phosphotyrosine-independent ligand of the p56lck SH2 domain. *Proceedings of the National Academy of Sciences of the United States of America* 93:5991-5995.

Karanasios, E., S.A. Walker, H. Okkenhaug, M. Manifava, E. Hummel, H. Zimmermann, Q. Ahmed, M.C. Domart, L. Collinson, and N.T. Ktistakis. 2016. Autophagy initiation by ULK complex assembly on ER tubulovesicular regions marked by ATG9 vesicles. *Nature communications* 7:12420.

Karvela, M., P. Baquero, E.M. Kuntz, A. Mukhopadhyay, R. Mitchell, E.K. Allan, E. Chan, K.R. Kranc, B. Calabretta, P. Salomoni, E. Gottlieb, T.L. Holyoake, and G.V. Helgason. 2016. ATG7 regulates energy metabolism, differentiation and survival of Philadelphia-chromosome-positive cells. *Autophagy* 12:936-948.

Khaminets, A., T. Heinrich, M. Mari, P. Grumati, A.K. Huebner, M. Akutsu, L. Liebmann, A. Stolz, S. Nietzsche, N. Koch, M. Mauthe, I. Katona, B. Qualmann, J. Weis, F. Reggiori, I. Kurth, C.A. Hubner, and I. Dikic. 2015. Regulation of endoplasmic reticulum turnover by selective autophagy. *Nature* 522:354-358.

Kim, I., S. Rodriguez-Enriquez, and J.J. Lemasters. 2007. Selective degradation of mitochondria by mitophagy. *Archives of biochemistry and biophysics* 462:245-253.

Kirkin, V., T. Lamark, T. Johansen, and I. Dikic. 2009a. NBR1 cooperates with p62 in selective autophagy of ubiquitinated targets. *Autophagy* 5:732-733.

8. References

Kirkin, V., T. Lamark, Y.S. Sou, G. Bjorkoy, J.L. Nunn, J.A. Bruun, E. Shvets, D.G. McEwan, T.H. Clausen, P. Wild, I. Bilusic, J.P. Theurillat, A. Overvatn, T. Ishii, Z. Elazar, M. Komatsu, I. Dikic, and T. Johansen. 2009b. A role for NBR1 in autophagosomal degradation of ubiquitinated substrates. *Molecular cell* 33:505-516.

Klionsky, D.J. 2008. Autophagy revisited: a conversation with Christian de Duve. *Autophagy* 4:740-743.

Komatsu, M., and Y. Ichimura. 2010. Selective autophagy regulates various cellular functions. *Genes to cells : devoted to molecular & cellular mechanisms* 15:923-933.

Kovac, S., P.R. Angelova, K.M. Holmstrom, Y. Zhang, A.T. Dinkova-Kostova, and A.Y. Abramov. 2015. Nrf2 regulates ROS production by mitochondria and NADPH oxidase. *Biochimica et biophysica acta* 1850:794-801.

Lam, H.C., C.V. Baglini, A.L. Lope, A.A. Parkhitko, H.J. Liu, N. Alesi, I.A. Malinowska, D. Ebrahimi-Fakhari, A. Saffari, J.J. Yu, A. Pereira, D. Khabibullin, B. Ogorek, J. Nijmeh, T. Kavanagh, A. Handen, S.Y. Chan, J.M. Asara, W.M. Oldham, M.T. Diaz-Meco, J. Moscat, M. Sahin, C. Priolo, and E.P. Henske. 2017. p62/SQSTM1 Cooperates with Hyperactive mTORC1 to Regulate Glutathione Production, Maintain Mitochondrial Integrity, and Promote Tumorigenesis. *Cancer research* 77:3255-3267.

Lamark, T., M. Perander, H. Outzen, K. Kristiansen, A. Overvatn, E. Michaelsen, G. Bjorkoy, and T. Johansen. 2003. Interaction codes within the family of mammalian Phox and Bem1p domain-containing proteins. *The Journal of biological chemistry* 278:34568-34581.

Laplante, M., and D.M. Sabatini. 2009. mTOR signaling at a glance. *Journal of cell science* 122:3589-3594.

Lazarou, M., D.A. Sliter, L.A. Kane, S.A. Sarraf, C. Wang, J.L. Burman, D.P. Sideris, A.I. Fogel, and R.J. Youle. 2015. The ubiquitin kinase PINK1 recruits autophagy receptors to induce mitophagy. *Nature* 524:309-314.

Lazova, R., R.L. Camp, V. Klump, S.F. Siddiqui, R.K. Amaravadi, and J.M. Pawelek. 2012. Punctate LC3B expression is a common feature of solid

8. References

tumors and associated with proliferation, metastasis, and poor outcome. *Clinical cancer research : an official journal of the American Association for Cancer Research* 18:370-379.

Lee, E.A., L. Angka, S.G. Rota, T. Hanlon, A. Mitchell, R. Hurren, X.M. Wang, M. Gronda, E. Boyaci, B. Bojko, M. Minden, S. Sriskanthadevan, A. Datti, J.L. Wrana, A. Edginton, J. Pawliszyn, J.W. Joseph, J. Quadrilatero, A.D. Schimmer, and P.A. Spagnuolo. 2015. Targeting Mitochondria with Avocatin B Induces Selective Leukemia Cell Death. *Cancer research* 75:2478-2488.

Lemasters, J.J. 2005. Selective mitochondrial autophagy, or mitophagy, as a targeted defense against oxidative stress, mitochondrial dysfunction, and aging. *Rejuvenation research* 8:3-5.

Levine, B., and G. Kroemer. 2008. Autophagy in the pathogenesis of disease. *Cell* 132:27-42.

Ley, T.J., C. Miller, L. Ding, B.J. Raphael, A.J. Mungall, A. Robertson, K. Hoadley, T.J. Triche, Jr., P.W. Laird, J.D. Baty, L.L. Fulton, R. Fulton, S.E. Heath, J. Kalicki-Veizer, C. Kandoth, J.M. Klco, D.C. Koboldt, K.L. Kanchi, S. Kulkarni, T.L. Lamprecht, D.E. Larson, L. Lin, C. Lu, M.D. McLellan, J.F. McMichael, J. Payton, H. Schmidt, D.H. Spencer, M.H. Tomasson, J.W. Wallis, L.D. Wartman, M.A. Watson, J. Welch, M.C. Wendl, A. Ally, M. Balasundaram, I. Birol, Y. Butterfield, R. Chiu, A. Chu, E. Chuah, H.J. Chun, R. Corbett, N. Dhalla, R. Guin, A. He, C. Hirst, M. Hirst, R.A. Holt, S. Jones, A. Karsan, D. Lee, H.I. Li, M.A. Marra, M. Mayo, R.A. Moore, K. Mungall, J. Parker, E. Pleasance, P. Plettner, J. Schein, D. Stoll, L. Swanson, A. Tam, N. Thiessen, R. Varhol, N. Wye, Y. Zhao, S. Gabriel, G. Getz, C. Sougnez, L. Zou, M.D. Leiserson, F. Vandin, H.T. Wu, F. Applebaum, S.B. Baylin, R. Akbani, B.M. Broom, K. Chen, T.C. Motter, K. Nguyen, J.N. Weinstein, N. Zhang, M.L. Ferguson, C. Adams, A. Black, J. Bowen, J. Gastier-Foster, T. Grossman, T. Lichtenberg, L. Wise, T. Davidsen, J.A. Demchok, K.R. Shaw, M. Sheth, H.J. Sofia, L. Yang, J.R. Downing, and G. Eley. 2013. Genomic and epigenomic landscapes of adult de novo acute myeloid leukemia. *The New England journal of medicine* 368:2059-2074.

8. References

Linares, J.F., A. Duran, M. Reina-Campos, P. Aza-Blanc, A. Campos, J. Moscat, and M.T. Diaz-Meco. 2015. Amino Acid Activation of mTORC1 by a PB1-Domain-Driven Kinase Complex Cascade. *Cell reports* 12:1339-1352.

Mann, M. 2006. Functional and quantitative proteomics using SILAC. *Nature reviews. Molecular cell biology* 7:952-958.

Mathew, R., C.M. Karp, B. Beaudoin, N. Vuong, G. Chen, H.Y. Chen, K. Bray, A. Reddy, G. Bhanot, C. Gelinas, R.S. Dipaola, V. Karantza-Wadsworth, and E. White. 2009. Autophagy suppresses tumorigenesis through elimination of p62. *Cell* 137:1062-1075.

Matsumoto, G., T. Shimogori, N. Hattori, and N. Nukina. 2015. TBK1 controls autophagosomal engulfment of polyubiquitinated mitochondria through p62/SQSTM1 phosphorylation. *Human molecular genetics* 24:4429-4442.

Mikkola, H.K., and S.H. Orkin. 2006. The journey of developing hematopoietic stem cells. *Development* 133:3733-3744.

Mizumura, K., A.M. Choi, and S.W. Ryter. 2014. Emerging role of selective autophagy in human diseases. *Front Pharmacol* 5:244.

Mizushima, N. 2007. Autophagy: process and function. *Genes & development* 21:2861-2873.

Mizushima, N., and T. Yoshimori. 2007. How to interpret LC3 immunoblotting. *Autophagy* 3:542-545.

Mortensen, M., E.J. Soilleux, G. Djordjevic, R. Tripp, M. Lutteropp, E. Sadighi-Akha, A.J. Stranks, J. Glanville, S. Knight, S.E. Jacobsen, K.R. Kranc, and A.K. Simon. 2011. The autophagy protein Atg7 is essential for hematopoietic stem cell maintenance. *The Journal of experimental medicine* 208:455-467.

Moscat, J., M. Karin, and M.T. Diaz-Meco. 2016. p62 in Cancer: Signaling Adaptor Beyond Autophagy. *Cell* 167:606-609.

Muller, T.D., S.J. Lee, M. Jastroch, D. Kabra, K. Stemmer, M. Aichler, B. Abplanalp, G. Ananthakrishnan, N. Bhardwaj, S. Collins, S. Divanovic, M. Endele, B. Finan, Y. Gao, K.M. Habegger, J. Hembree, K.M. Heppner, S.

8. References

Hofmann, J. Holland, D. Kuchler, M. Kutschke, R. Krishna, M. Lehti, R. Oelkrug, N. Ottaway, D. Perez-Tilve, C. Raver, A.K. Walch, S.C. Schriever, J. Speakman, Y.H. Tseng, M. Diaz-Meco, P.T. Pfluger, J. Moscat, and M.H. Tschop. 2013. p62 links beta-adrenergic input to mitochondrial function and thermogenesis. *The Journal of clinical investigation* 123:469-478.

Murphy, M.P. 2013. Mitochondrial dysfunction indirectly elevates ROS production by the endoplasmic reticulum. *Cell metabolism* 18:145-146.

Narendra, D., L.A. Kane, D.N. Hauser, I.M. Fearnley, and R.J. Youle. 2010a. p62/SQSTM1 is required for Parkin-induced mitochondrial clustering but not mitophagy; VDAC1 is dispensable for both. *Autophagy* 6:1090-1106.

Narendra, D.P., S.M. Jin, A. Tanaka, D.F. Suen, C.A. Gautier, J. Shen, M.R. Cookson, and R.J. Youle. 2010b. PINK1 is selectively stabilized on impaired mitochondria to activate Parkin. *PLoS biology* 8:e1000298.

Noda, N.N., Y. Ohsumi, and F. Inagaki. 2009. ATG systems from the protein structural point of view. *Chemical reviews* 109:1587-1598.

Novak, I., V. Kirkin, D.G. McEwan, J. Zhang, P. Wild, A. Rozenknop, V. Rogov, F. Lohr, D. Popovic, A. Occhipinti, A.S. Reichert, J. Terzic, V. Dotsch, P.A. Ney, and I. Dikic. 2010. Nix is a selective autophagy receptor for mitochondrial clearance. *EMBO reports* 11:45-51.

Oellerich, T., M.F. Oellerich, M. Engelke, S. Munch, S. Mohr, M. Nimz, H.H. Hsiao, J. Corso, J. Zhang, H. Bohnenberger, T. Berg, M.A. Rieger, J. Wienands, G. Bug, C. Brandts, H. Urlaub, and H. Serve. 2013. beta2 integrin-derived signals induce cell survival and proliferation of AML blasts by activating a Syk/STAT signaling axis. *Blood* 121:3889-3899, S3881-3866.

Okatsu, K., K. Saisho, M. Shimanuki, K. Nakada, H. Shitara, Y.S. Sou, M. Kimura, S. Sato, N. Hattori, M. Komatsu, K. Tanaka, and N. Matsuda. 2010. p62/SQSTM1 cooperates with Parkin for perinuclear clustering of depolarized mitochondria. *Genes to cells : devoted to molecular & cellular mechanisms* 15:887-900.

Pankiv, S., T.H. Clausen, T. Lamark, A. Brech, J.A. Bruun, H. Outzen, A. Overvatn, G. Bjorkoy, and T. Johansen. 2007. p62/SQSTM1 binds directly to

8. References

Atg8/LC3 to facilitate degradation of ubiquitinated protein aggregates by autophagy. *The Journal of biological chemistry* 282:24131-24145.

Piva, R., G. Belardo, and M.G. Santoro. 2006. NF-kappaB: a stress-regulated switch for cell survival. *Antioxidants & redox signaling* 8:478-486.

Qu, X., J. Yu, G. Bhagat, N. Furuya, H. Hibshoosh, A. Troxel, J. Rosen, E.L. Eskelinen, N. Mizushima, Y. Ohsumi, G. Cattoretti, and B. Levine. 2003. Promotion of tumorigenesis by heterozygous disruption of the beclin 1 autophagy gene. *The Journal of clinical investigation* 112:1809-1820.

Rakovic, A., K. Shurkewitsch, P. Seibler, A. Grunewald, A. Zanon, J. Hagenah, D. Krainc, and C. Klein. 2013. Phosphatase and tensin homolog (PTEN)-induced putative kinase 1 (PINK1)-dependent ubiquitination of endogenous Parkin attenuates mitophagy: study in human primary fibroblasts and induced pluripotent stem cell-derived neurons. *The Journal of biological chemistry* 288:2223-2237.

Rao, S., L. Tortola, T. Perlot, G. Wirnsberger, M. Novatchkova, R. Nitsch, P. Sykacek, L. Frank, D. Schramek, V. Komnenovic, V. Sigl, K. Aumayr, G. Schmauss, N. Fellner, S. Handschuh, M. Glosmann, P. Pasierbek, M. Schlederer, G.P. Resch, Y. Ma, H. Yang, H. Popper, L. Kenner, G. Kroemer, and J.M. Penninger. 2014. A dual role for autophagy in a murine model of lung cancer. *Nature communications* 5:3056.

Rao, X., X. Huang, Z. Zhou, and X. Lin. 2013. An improvement of the 2^(-delta delta CT) method for quantitative real-time polymerase chain reaction data analysis. *Biostatistics, bioinformatics and biomathematics* 3:71-85.

Ren, F., G. Shu, G. Liu, D. Liu, J. Zhou, and L. Yuan. 2014. Knockdown of p62/sequestosome 1 attenuates autophagy and inhibits colorectal cancer cell growth. *Molecular and cellular biochemistry* 385:95-102.

Ribas, V., C. Garcia-Ruiz, and J.C. Fernandez-Checa. 2014. Glutathione and mitochondria. *Frontiers in pharmacology* 5:151.

Richter, B., D.A. Sliter, L. Herhaus, A. Stolz, C. Wang, P. Beli, G. Zaffagnini, P. Wild, S. Martens, S.A. Wagner, R.J. Youle, and I. Dikic. 2016. Phosphorylation of OPTN by TBK1 enhances its binding to Ub chains and

promotes selective autophagy of damaged mitochondria. *Proceedings of the National Academy of Sciences of the United States of America* 113:4039-4044.

Rosenfeldt, M.T., J. O'Prey, J.P. Morton, C. Nixon, G. MacKay, A. Mrowinska, A. Au, T.S. Rai, L. Zheng, R. Ridgway, P.D. Adams, K.I. Anderson, E. Gottlieb, O.J. Sansom, and K.M. Ryan. 2013. p53 status determines the role of autophagy in pancreatic tumour development. *Nature* 504:296-300.

Russell, R.C., Y. Tian, H. Yuan, H.W. Park, Y.Y. Chang, J. Kim, H. Kim, T.P. Neufeld, A. Dillin, and K.L. Guan. 2013. ULK1 induces autophagy by phosphorylating Beclin-1 and activating VPS34 lipid kinase. *Nature cell biology* 15:741-750.

Sanchez, P., G. De Carcer, I.V. Sandoval, J. Moscat, and M.T. Diaz-Meco. 1998. Localization of atypical protein kinase C isoforms into lysosome-targeted endosomes through interaction with p62. *Molecular and cellular biology* 18:3069-3080.

Sanz, L., M.T. Diaz-Meco, H. Nakano, and J. Moscat. 2000. The atypical PKC-interacting protein p62 channels NF-kappaB activation by the IL-1-TRAF6 pathway. *The EMBO journal* 19:1576-1586.

Sarraf, S.A., M. Raman, V. Guarani-Pereira, M.E. Sowa, E.L. Huttlin, S.P. Gygi, and J.W. Harper. 2013. Landscape of the PARKIN-dependent ubiquitylome in response to mitochondrial depolarization. *Nature* 496:372-376.

Schlenk, R.F. 2014. Post-remission therapy for acute myeloid leukemia. *Haematologica* 99:1663-1670.

Schweers, R.L., J. Zhang, M.S. Randall, M.R. Loyd, W. Li, F.C. Dorsey, M. Kundu, J.T. Opferman, J.L. Cleveland, J.L. Miller, and P.A. Ney. 2007. NIX is required for programmed mitochondrial clearance during reticulocyte maturation. *Proceedings of the National Academy of Sciences of the United States of America* 104:19500-19505.

8. References

Seibenhener, M.L., Y. Du, M.T. Diaz-Meco, J. Moscat, M.C. Wooten, and M.W. Wooten. 2013. A role for sequestosome 1/p62 in mitochondrial dynamics, import and genome integrity. *Biochimica et biophysica acta* 1833:452-459.

Shaid, S., C.H. Brandts, H. Serve, and I. Dikic. 2013. Ubiquitination and selective autophagy. *Cell death and differentiation* 20:21-30.

Shubin, A.V., I.V. Demidyuk, A.A. Komissarov, L.M. Rafieva, and S.V. Kostrov. 2016. Cytoplasmic vacuolization in cell death and survival. *Oncotarget* 7:55863-55889.

Skrtic, M., S. Sriskanthadevan, B. Jhas, M. Gebbia, X. Wang, Z. Wang, R. Hurren, Y. Jitkova, M. Gronda, N. Maclean, C.K. Lai, Y. Eberhard, J. Bartoszko, P. Spagnuolo, A.C. Rutledge, A. Datti, T. Ketela, J. Moffat, B.H. Robinson, J.H. Cameron, J. Wrana, C.J. Eaves, M.D. Minden, J.C. Wang, J.E. Dick, K. Humphries, C. Nislow, G. Giaever, and A.D. Schimmer. 2011. Inhibition of mitochondrial translation as a therapeutic strategy for human acute myeloid leukemia. *Cancer cell* 20:674-688.

Strohecker, A.M., J.Y. Guo, G. Karsli-Uzunbas, S.M. Price, G.J. Chen, R. Mathew, M. McMahon, and E. White. 2013. Autophagy sustains mitochondrial glutamine metabolism and growth of BrafV600E-driven lung tumors. *Cancer discovery* 3:1272-1285.

Sullivan, L.B., and N.S. Chandel. 2014. Mitochondrial reactive oxygen species and cancer. *Cancer & metabolism* 2:17.

Sumitomo, Y., J. Koya, K. Nakazaki, K. Kataoka, T. Tsuruta-Kishino, K. Morita, T. Sato, and M. Kurokawa. 2016. Cytoprotective autophagy maintains leukemia-initiating cells in murine myeloid leukemia. *Blood* 128:1614-1624.

Sutovsky, P., R.D. Moreno, J. Ramalho-Santos, T. Dominko, C. Simerly, and G. Schatten. 1999. Ubiquitin tag for sperm mitochondria. *Nature* 402:371-372.

Tabe, Y., and M. Konopleva. 2014. Advances in understanding the leukaemia microenvironment. *British journal of haematology* 164:767-778.

8. References

Takamura, A., M. Komatsu, T. Hara, A. Sakamoto, C. Kishi, S. Waguri, Y. Eishi, O. Hino, K. Tanaka, and N. Mizushima. 2011. Autophagy-deficient mice develop multiple liver tumors. *Genes & development* 25:795-800.

Thurston, T.L., M.P. Wandel, N. von Muhlinen, A. Foeglein, and F. Randow. 2012. Galectin 8 targets damaged vesicles for autophagy to defend cells against bacterial invasion. *Nature* 482:414-418.

Tolkovsky, A.M., L. Xue, G.C. Fletcher, and V. Borutaite. 2002. Mitochondrial disappearance from cells: a clue to the role of autophagy in programmed cell death and disease? *Biochimie* 84:233-240.

Trocoli, A., P. Bensadoun, E. Richard, G. Labrunie, F. Merhi, A.M. Schlafli, D. Brigger, S. Souquere, G. Pierron, J.M. Pasquet, P. Soubeyran, J. Reiffers, E. Segal-Bendirdjian, M.P. Tschan, and M. Djavaheri-Mergny. 2014. p62/SQSTM1 upregulation constitutes a survival mechanism that occurs during granulocytic differentiation of acute myeloid leukemia cells. *Cell death and differentiation* 21:1852-1861.

Turrens, J.F. 2003. Mitochondrial formation of reactive oxygen species. *The Journal of physiology* 552:335-344.

Twig, G., A. Elorza, A.J. Molina, H. Mohamed, J.D. Wikstrom, G. Walzer, L. Stiles, S.E. Haigh, S. Katz, G. Las, J. Alroy, M. Wu, B.F. Py, J. Yuan, J.T. Deeney, B.E. Corkey, and O.S. Shirihai. 2008. Fission and selective fusion govern mitochondrial segregation and elimination by autophagy. *The EMBO journal* 27:433-446.

Umemura, A., F. He, K. Taniguchi, H. Nakagawa, S. Yamachika, J. Font-Burgada, Z. Zhong, S. Subramaniam, S. Raghunandan, A. Duran, J.F. Linares, M. Reina-Campos, S. Umemura, M.A. Valasek, E. Seki, K. Yamaguchi, K. Koike, Y. Itoh, M.T. Diaz-Meco, J. Moscat, and M. Karin. 2016. p62, Upregulated during Preneoplasia, Induces Hepatocellular Carcinogenesis by Maintaining Survival of Stressed HCC-Initiating Cells. *Cancer cell* 29:935-948.

Visconte, V., B. Przychodzen, Y. Han, S.T. Nawrocki, S. Thota, K.R. Kelly, B.J. Patel, C. Hirsch, A.S. Advani, H.E. Carraway, M.A. Sekeres, J.P.

8. References

Maciejewski, and J.S. Carew. 2017. Complete mutational spectrum of the autophagy interactome: a novel class of tumor suppressor genes in myeloid neoplasms. *Leukemia* 31:505-510.

Wang, K., and D.J. Klionsky. 2011. Mitochondria removal by autophagy. *Autophagy* 7:297-300.

Wang, X., Z. Du, L. Li, M. Shi, and Y. Yu. 2015. Beclin 1 and p62 expression in non-small cell lung cancer: relation with malignant behaviors and clinical outcome. *International journal of clinical and experimental pathology* 8:10644-10652.

Warr, M.R., M. Binnewies, J. Flach, D. Reynaud, T. Garg, R. Malhotra, J. Debnath, and E. Passegue. 2013. FOXO3A directs a protective autophagy program in haematopoietic stem cells. *Nature* 494:323-327.

Weidberg, H., T. Shpilka, E. Shvets, A. Abada, F. Shimron, and Z. Elazar. 2011. LC3 and GATE-16 N termini mediate membrane fusion processes required for autophagosome biogenesis. *Developmental cell* 20:444-454.

Weissman, I.L. 2000. Stem cells: units of development, units of regeneration, and units in evolution. *Cell* 100:157-168.

White, E. 2012. Deconvoluting the context-dependent role for autophagy in cancer. *Nature reviews. Cancer* 12:401-410.

Wild, P., H. Farhan, D.G. McEwan, S. Wagner, V.V. Rogov, N.R. Brady, B. Richter, J. Korac, O. Waidmann, C. Choudhary, V. Dotsch, D. Bumann, and I. Dikic. 2011. Phosphorylation of the autophagy receptor optineurin restricts Salmonella growth. *Science* 333:228-233.

Wooten, M.W., M.L. Seibenhener, V. Mamidipudi, M.T. Diaz-Meco, P.A. Barker, and J. Moscat. 2001. The atypical protein kinase C-interacting protein p62 is a scaffold for NF-kappaB activation by nerve growth factor. *The Journal of biological chemistry* 276:7709-7712.

Yang, A., N.V. Rajeshkumar, X. Wang, S. Yabuuchi, B.M. Alexander, G.C. Chu, D.D. Von Hoff, A. Maitra, and A.C. Kimmelman. 2014. Autophagy is

critical for pancreatic tumor growth and progression in tumors with p53 alterations. *Cancer discovery* 4:905-913.

Youle, R.J., and D.P. Narendra. 2011. Mechanisms of mitophagy. *Nature reviews. Molecular cell biology* 12:9-14.

Zhang, J., and P.A. Ney. 2009. Role of BNIP3 and NIX in cell death, autophagy, and mitophagy. *Cell death and differentiation* 16:939-946.

Zhang, J., D.N. Tripathi, J. Jing, A. Alexander, J. Kim, R.T. Powell, R. Dere, J. Tait-Mulder, J.H. Lee, T.T. Paull, R.K. Pandita, V.K. Charaka, T.K. Pandita, M.B. Kastan, and C.L. Walker. 2015. ATM functions at the peroxisome to induce pexophagy in response to ROS. *Nature cell biology* 17:1259-1269.

Zorov, D.B., M. Juhaszova, and S.J. Sollott. 2014. Mitochondrial reactive oxygen species (ROS) and ROS-induced ROS release. *Physiol Rev* 94:909-950.

9. Abbreviations

7AAD	7-Aminoactinomycin D
AML	Acute myeloid leukemia
aPKCs	Atypical protein kinase C isoforms
ATG	Autophagy-related genes
ATRA	all-trans retinoic acid
BSA	Bovine serum albumin
BM	Bone marrow
Baf	Bafilomycin A1
BFP	Blue fluorescent protein
BrdU	Bromodeoxyuridine
CR	Complete remission
CMA	Chaperone-mediated autophagy
Crp62	CRISPR/Cas9 targeting human p62
CrNTC	CRISPR/Cas9 targeting human non-targeting control
CMP	Common myeloid progenitors
CCCP	Carbonyl cyanide m‑chlorophenylhydrazone
COXIV	Cytochrome C oxidase subunit IV
CML	Chronic myeloid leukemia
cDNA	Complementary DNA
Ct	Threshold cycle
DFP	Deferiprone
ER	Endoplasmic reticulum
FCS	Fetal calf serum
FBS	Fetal bovine serum

9. Abbreviations

GFP	Green fluorescent protein
GMP	Granulocyte macrophage progenitors
gRNAs	guide RNAs
HSC	Hematopoietic stem cell
HEK-293	Human embryonic kidney cell 293
HCC	Hepatocellular carcinoma
H	Heavy
HRP	Horseradish peroxidase
IDH2	Isocitrate dehydrogenases
KIR	Keap1-interaction region
ldMBM	Lineage-depleted mouse bone marrow
Lin	Lineage
LIR	LC3-interacting region
LT-HSC	Long-term hematopoietic stem cells
L	Light
LICs	Leukemia-initiating cells
LC3	microtubule associated protein 1 light-chain 3
mSCF	Murine stem cell factor
mIL-3	Murine interleukin-3
mIL-6	Murine interleukin-6
mTOR	Mammalian target of rapamycin
MOM	Mitochondrial outer membrane
M	Medium
MPP	Multipotent progenitors
MN1	Meningioma 1
MEF	Mouse embryonic fibroblast

9. Abbreviations

NBR1	Neighbour of BRCA1
NDP52	Nuclear dot protein 52
OPTN	Optineurin
$O^{2-\bullet}$	Superoxide anion
OCR	Oxygen consumption rate
Plat-E	Platinum-E retroviral packaging cell line
p62/SQSTM1	Sequestosome 1
PKC	Protein kinase C
Pen Strep	Penicillin and streptomycin
PBS	Phosphate buffered saline
PB1	Phox and Bem1
PLT	Platelet
PEI	Polyethylenimine
PBST	PBS and 0.1% Tween® 20
RBC	Red blood cell
ROS	Reactive oxygen species
RT	Room temperature
RT-PCR	Reverse transcription polymerase chain reaction
shRNA	Short-hairpin RNA
shp62	shRNA against mouse p62
shCtrl	shRNA against mouse non-targeting control
ST-HSC	Short-term hematopoietic stem cells
SEM	Standard error of the mean
SILAC	Stable isotope labeling with amino acids in cell culture
SOD	Superoxide dismutase
TNF	Tumor necrosis factor

9. Abbreviations

TRAF6	Tumor necrosis factor receptor associated factor 6
TB	TRAF6-binding
UBD	Ubiquitination-binding domain
UBA	Ubiquitin-associated
UBAN	Ubiquitin binding in ABIN and NEMO
UBZ	Ubiquitin-binding zinc finger
WBC	White blood cell
WT	Wildtype

10. Eidesstattliche Erklärung

Hiermit erkläre ich an Eides statt, dass ich die vorliegende Dissertation selbständig und ohne unerlaubte Hilfe angefertigt und andere als die in der Arbeit angegebenen Hilfsmittel nicht benutzt habe. Alle Stellen, die wörtlich oder sinngemäß aus anderen Schriften entnommen werden, habe ich als solche kenntlich gemacht. Diese Arbeit hat in der gleichen oder ähnlichen Form noch keiner Prüfungsbehörde vorgelegen. Des Weiteren bin ich mit der späteren Ausleihe meiner Doktorarbeit an die Fachbereichsbibliothek einverstanden.

Frankfurt, den 23.10.2017

The Duy Nguyen